

South Dakota State University

# Open PRAIRIE: Open Public Research Access Institutional Repository and Information Exchange

---

Electronic Theses and Dissertations

---

1971

## Nonlinear System Identification Using an Analog Technique

G. N. Govindan

Follow this and additional works at: <https://openprairie.sdstate.edu/etd>

---

### Recommended Citation

Govindan, G. N., "Nonlinear System Identification Using an Analog Technique" (1971). *Electronic Theses and Dissertations*. 3716.

<https://openprairie.sdstate.edu/etd/3716>

This Thesis - Open Access is brought to you for free and open access by Open PRAIRIE: Open Public Research Access Institutional Repository and Information Exchange. It has been accepted for inclusion in Electronic Theses and Dissertations by an authorized administrator of Open PRAIRIE: Open Public Research Access Institutional Repository and Information Exchange. For more information, please contact [michael.biondo@sdstate.edu](mailto:michael.biondo@sdstate.edu).

NONLINEAR SYSTEM IDENTIFICATION  
USING AN ANALOG TECHNIQUE

BY

G. N. GOVINDAN

A thesis submitted  
in partial fulfillment of the requirements for the  
degree Master of Science, Department of  
Electrical Engineering, South Dakota  
State University

1971


SOUTH DAKOTA STATE UNIVERSITY LIBRARY

NONLINEAR SYSTEM IDENTIFICATION

USING AN ANALOG TECHNIQUE

This thesis is approved as a creditable and independent investigation by a candidate for the degree, Master of Science, and is acceptable as meeting the thesis requirements for this degree, but without implying that the conclusions reached by the candidate are necessarily the conclusions of the major department.

---

R. A. Higgins   
Thesis Adviser

Date

F. C. Fitchen, Head  
Electrical Engineering Department

Date

## ACKNOWLEDGEMENTS

The author wishes to express his appreciation and gratitude to Dr. R. A. Higgins, whose guidance and advice made this investigation possible, to Dr. F. C. Fitchen for the valuable help rendered, and to Mrs. Janice Sills for typing the first draft and final copy of this thesis.

TABLE OF CONTENTS

CHAPTER	PAGE
I. INTRODUCTION . . . . .	1
II. Kohr'S METHOD OF IDENTIFYING SIMPLE NONLINEAR SYSTEMS . . .	5
III. APPLICATION OF KOHR'S METHOD TO SYSTEMS CONTAINING SINGLE-VALUED NONLINEARITIES . . . . .	21
A. Limiting element in a first-order system . . . . .	21
B. Dead zone element in a first-order system . . . . .	32
C. Relay element in a first-order system . . . . .	39
IV. KOHR'S METHOD APPLIED TO SYSTEMS CONTAINING DOUBLE-VALUED NONLINEARITIES . . . . .	42
V. DETERMINATION OF THE ORDER OF THE SYSTEM . . . . .	50
VI. CONCLUSIONS . . . . .	60
REFERENCES . . . . .	64
APPENDIX A . . . . .	67
APPENDIX B . . . . .	69
APPENDIX C . . . . .	80

LIST OF TABLES

TABLE	PAGE
1. The Minimum ITAE Standard Forms, Zero-Displacement Error Systems. . . . .	80
2. The Butterworth Standard Forms. . . . .	80

## LIST OF FIGURES

FIGURE	PAGE
2-1. Exact calculation of a nonlinear function. . . . .	7
2-2. Mechanization of a filter to provide derivatives of the output. . . . .	10
2-3. Practical calculation of a nonlinear function. . . . .	11
3-1. Simulated limiting type nonlinearity. . . . .	22
3-2. Calculated nonlinear function (limiting) for $\omega = 0.75$ rad/sec, and $a_1 = 1.0$ . . . . .	23
3-3. Calculated nonlinear function (limiting) for $\omega = 0.5$ rad/sec, and $a_1 = 1.0$ . . . . .	24
3-4. Calculated nonlinear function (limiting) for $\omega = 0.25$ rad/sec, and $a_1 = 1.0$ . . . . .	25
3-5. Calculated nonlinear function (limiting) for $\omega = 0.1$ rad/sec, and $a_1 = 1.0$ . . . . .	26
3-6. Calculated nonlinear function (limiting) for $\omega = 0.1$ rad/sec, and $a_1 = 1.25$ . . . . .	28
3-7. Calculated nonlinear function (limiting) for $\omega = 0.1$ rad/sec, and $a_1 = 1.5$ . . . . .	29
3-8. Calculated nonlinear function (limiting) for $\omega = 0.1$ rad/sec, and $a_1 = 0.75$ . . . . .	30
3-9. Calculated nonlinear function (limiting) for $\omega = 0.1$ rad/sec, and $a_1 = 0.5$ . . . . .	31
3-10. Simulated dead zone type nonlinearity . . . . .	33
3-11. Calculated nonlinear function (dead zone) for $\omega = 0.1$ rad/sec, and $a_1 = 1.0$ . . . . .	34
3-12. Calculated nonlinear function (deadzone) for $\omega = 0.1$ rad/sec, and $a_1 = 1.25$ . . . . .	35
3-13. Calculated nonlinear function (dead zone) for $\omega = 0.1$ rad/sec, and $a_1 = 1.5$ . . . . .	36

FIGURE	PAGE
3-14. Calculated nonlinear function (dead zone) for $\omega = 0.1$ rad/sec, and $a_1 = 0.75$ . . . . .	37
3-15. Calculated nonlinear function (dead zone) for $\omega = 0.1$ rad/sec, and $a_1 = 0.5$ . . . . .	38
3-16. Simulated relay type nonlinearity. . . . .	40
3-17. Calculated nonlinear function (relay) for $\omega = 0.1$ rad/sec and $a_1 = 1.0$ . . . . .	41
4-1. Simulated backlash type nonlinearity. . . . .	43
4-2. Calculated nonlinear function (backlash) for $\omega = 0.1$ rad/sec, and $a_1 = 2.0$ . . . . .	44
4-3. Calculated nonlinear function (backlash) for $\omega = 0.1$ rad/sec, and $a_1 = 1.5$ . . . . .	45
4-4. Calculated nonlinear function (backlash) for $\omega = 0.1$ rad/sec, and $a_1 = 1.0$ . . . . .	46
4-5. Calculated nonlinear function (backlash) for $\omega = 0.1$ rad/sec, and $a_1 = 0.5$ . . . . .	47
4-6. Calculated nonlinear function (backlash) for $\omega = 0.1$ rad/sec, and $a_1 = 0.0$ . . . . .	48
5-1. Calculated nonlinear function for $b_1 = 2.0$ , $b_2 = 2.0$ , and $b_3 = 2.0$ . . . . .	53
5-2. Calculated nonlinear function for $b_1 = 1.0$ , $b_2 = 2.0$ , and $b_3 = 2.0$ . . . . .	54
5-3. Calculated nonlinear function for $b_1 = 1.0$ , $b_2 = 0.0$ , and $b_3 = 2.0$ . . . . .	55
5-4. Calculated nonlinear function for $b_1 = 1.0$ , $b_2 = 0.0$ , and $b_3 = 0.0$ . . . . .	56
5-5. Calculated nonlinear function for $b_1 = 1.0$ , $b_2 = 1.0$ , and $b_3 = 1.0$ . . . . .	58
5-6. Calculated nonlinear function for $b_1 = 0.0$ , $b_2 = 0.0$ , and $b_3 = 0.0$ . . . . .	59
A-1. Simulation scheme for the identification of first-order nonlinear system. . . . .	68



FIGURE	PAGE
B-1. Simulation of limiting type nonlinearity. . . . .	70
B-2. Simulation of dead zone. . . . .	72
B-3. Simulation of Coulomb friction. . . . .	74
B-4. Simulation of backlash. . . . .	76
B-5. Simulation of relay with hysteresis. . . . .	79

## CHAPTER I

### INTRODUCTION

The problem of identifying a black box - that is, determining its input-output relationships by experimental means - occurs under different guises in various branches of science. Some writers refer to it as the characterization problem. Others term it the measurement or the evaluation problem. Some - borrowing a term from physics - call it gedanken or thought experiments. In this work, the term "identification" is used since it seems to state the crux of the problem with greater clarity than the more standard terms cited above.

System characterization and system identification are basic problems in system theory. System characterization is primarily concerned with the setting up of mathematical models to represent input-output relationships; whereas system identification deals with the choice of a specific model from a class of models which is mathematically equivalent to a given physical system. For a specified input, this equivalence is established by comparing the outputs of both the system and the model to minimize some functional of the error. If the minimum of the functional is less than a predetermined value, the model and the system are considered equivalent.

While numerous methods exist for the identification of a linear system, there are very few practical techniques or methods available for the identification of systems containing nonlinear elements. This may be attributed partly to the fact that most of the analytic work in the area of nonlinear identification assumes the input to be a random

signal with prespecified properties, usually with white Gaussian noise. In practical situations, the identification has to be accomplished on the basis of existing input-output data, which may not fit the Gaussian assumption or other presupposed restrictions.

The methods that are presently available for practical identification of systems, which contain nonlinear elements, usually employ an ordinary differential equation as a model to describe the performance of the system.

Shinbrot<sup>1</sup> has presented a method for the determination of power series approximations to single-valued nonlinear functions in differential equations used to describe time-invariant systems. The accuracy of Shinbrot's method depends on the number of terms used in the power series as well as on the rapid convergence of the power series. Also, this method is limited to single-valued nonlinear functions.

Clymer<sup>2</sup> has proposed an implicit computation technique in which an unknown nonlinear function,  $f(x)$ , is used to characterize the nonlinear element. This function is then obtained directly for a given input,  $x$ . The computation is carried out by an implicit circuit which contains a mechanization of a differential equation which is complete except for the unknown nonlinear characteristic. This unknown characteristic is synthesized by an implicit circuit which continuously compares the values generated for the dependent variable with experimental time histories of the dependent variable, and which greatly amplifies the difference between them. This method is of value since a plot of the nonlinear characteristic may be obtained directly on an oscilloscope

or x-y plotter. But it is somewhat difficult to apply due to the problems encountered in stabilizing the implicit circuit.

Narendra and Gallman<sup>7</sup> proposed an iterative method for the identification of nonlinear systems from samples of inputs and outputs in the presence of noise. The model used for identification consists of a no memory gain (of an assumed polynomial form) followed by a linear discrete system. The parameters of the pulse transfer function of the linear system and the coefficients of the polynomial nonlinearity are alternately adjusted to minimize a mean-square error criterion. This method is restricted to single-valued nonlinearities and requires a digital computer for implementation.

R. H. Kohr<sup>3</sup> has given a method to obtain a graphical plot of an unknown nonlinear function versus its argument using analog computer when the system is time-invariant.

Giese and McGhee<sup>4</sup> and Detchmندی and Sridhar<sup>5</sup> present procedures which minimize "mean-squared error criteria" to estimate the unknown constants in an assumed nonlinear differential equation model. These procedures make use of a digital computer.

Hoerberock and Kohr<sup>10</sup> have evolved a method for determining an ordinary differential equation to describe the performance of a given lumped-parameter, time-invariant, nonlinear system having a single input and a single output. This technique utilizes a variation of the steepest descent method to minimize a model residue or error and the corresponding coefficients of the differential equation model which give zero or minimum error will be the calculated values of the

coefficients in the differential equation. This method may be implemented either on a digital computer or on an analog computer. This technique is based on the studies of Kohr<sup>3</sup> and Graupe<sup>6</sup> and incorporates some of the features of both these works. But this method is more difficult to implement on an analog computer than that of Kohr.

In the method given by Hoberock and Kohr, no definite class of input signals is specified which will enable complete identification of nonlinear systems. In Kohr's method, random inputs as well as periodic inputs may be used for identification. Both single-valued and double-valued (memory type) nonlinearities can be identified using this method. The method requires only an analog computer.

The prime purpose of this thesis project is to investigate and to implement Kohr's method. Kohr's method of identification was selected for study mainly because of the easy accessibility of the analog computer, in addition to the other advantages mentioned above.

In this thesis the method of Kohr is shown to apply to the identification of single-valued nonlinearities. However, it is also shown in the work to follow that the method does not apply, in general, to double-valued nonlinearities. Further, an extension of this method is developed herein which enables the determination of system order. A number of examples illustrating the implementation of the method, its restriction, and extension are given in the thesis.

## CHAPTER II

## KOHHR'S METHOD OF IDENTIFYING SIMPLE NONLINEAR SYSTEMS

The basic idea of Kohr<sup>3</sup> regarding the identification of simple nonlinear systems may be stated as follows:

Suppose that it is necessary to form the mathematical model, the differential equation, to represent a system, S. It is assumed that the system is composed of time-invariant, lumped parameter elements. The differential equation for the system may be obtained, if the following conditions are satisfied.

1. The input-output relationship of the system S may be accurately represented by an ordinary differential equation.
2. The system S contains a single nonlinear element which may be represented by a function of a single variable.
3. All coefficients of linear terms in the differential equation are known.

The problem of identifying multiple nonlinear elements and unknown linear coefficients will be considered in later paragraphs.

Let  $y$  be the input and  $x$  be the output of the system S. Also, let the system be represented by the differential equation,

$$a_n p^n x + a_{n-1} p^{n-1} x + \dots + a_{k+1} p^{k+1} x + f_k(p^k x) + a_{k-1} p^{k-1} x + \dots + a_1 p x + a_0 x = y, \quad (n \geq k \geq 0) \quad (1)$$

where

$$p^i x = \frac{d^i x}{dt^i}$$

$$a_i = \text{constant},$$

and the nonlinearity is indicated by the function  $f_k(p^k x)$ , meaning that the system contains an element whose performance may be represented by a nonlinear function of the  $k^{\text{th}}$  derivative of the output  $x$ . The nonlinear nature assumed for the function  $f_k(p^k x)$  does not preclude the possibility that the function may be entirely linear or, otherwise, that it may be composed of a sum of linear and nonlinear functions of  $p^k x$ . For convenience, it is assumed that the function  $f_k(p^k x)$  includes all functions of  $p^k x$ , linear or nonlinear, which appear in (1).

This equation may be solved for the nonlinear function by rearranging the differential equation as

$$f_k(p^k x) = y - (a_n p^n x + a_{n-1} p^{n-1} x + \dots + a_{k+1} p^{k+1} x + a_{k-1} p^{k-1} x + \dots + a_1 p x + a_0 x) \quad (2)$$

Thus it is clear from equation (2) that if the input  $y$ , the output  $x$ , together with its derivatives to the  $n^{\text{th}}$  order, and the linear coefficients  $a_j$  are all available, the function  $f_k(p^k x)$  may be computed directly. The characteristic curve for the nonlinear element is then obtained by plotting  $f_k(p^k x)$  versus  $p^k x$ . The procedure is illustrated in Fig. 2-1, in which the derivatives of the system output are obtained by a derivative computer.

For real physical systems, it is difficult to accomplish the scheme illustrated in Fig. 2-1 based on the calculation indicated by (2). The primary computational difficulties arise from the assumptions that an arbitrary number of derivatives of the output are available, that the coefficients of the linear terms in the differential equation are all known, and that the system contains only one nonlinear element. These

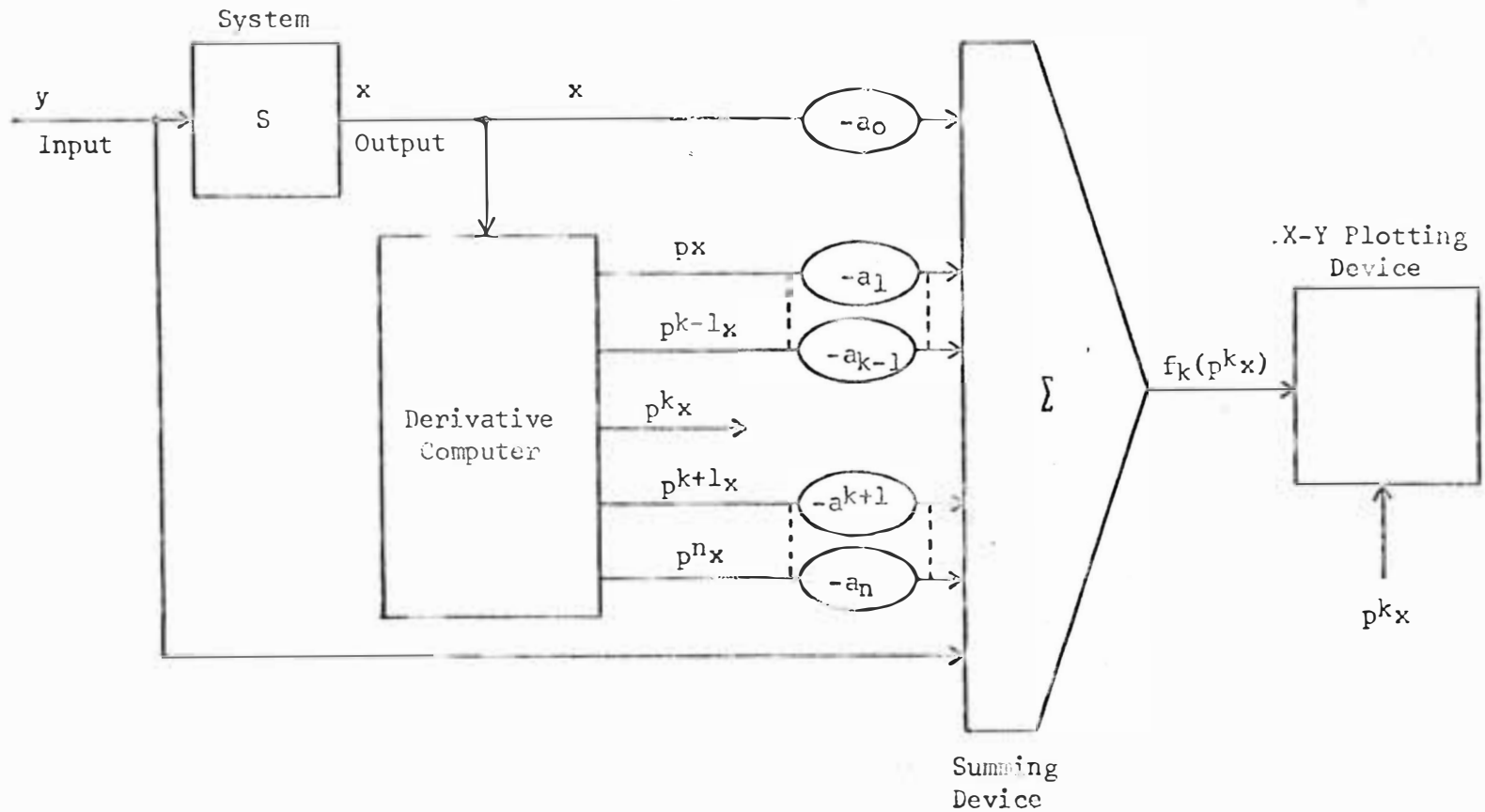


Fig. 2-1. Exact calculation of a nonlinear function.



three difficulties will be discussed and examined in material to follow.

The method of obtaining higher derivatives of the output from the output of physical system by direct differentiation, using differentiators, is ruled out since any true differentiator will greatly amplify the high frequency noise that may be present. The noise amplification problem becomes acute when a second or third differentiation is attempted. Hence, some other method should be chosen for obtaining the derivatives of the output of the physical system. This becomes imperative since no physical system is free from noise.

A method has been suggested by Mathews and Seifert<sup>8</sup> to obtain an arbitrary number of approximate derivatives from the output of the physical system. The method consists of constructing a linear filter in such a manner that there is available from it not only the filtered input signal, but also derivatives of the filtered input signal. The output of the physical system is the input to the linear filter. Thus the filtered output of the physical system and its derivatives can be obtained using this method.

In order to demonstrate one method of constructing such a filter, consider that the filter has an input,  $W$ , and an output,  $Z$ , which are related by

$$d_n p^n Z + d_{n-1} p^{n-1} Z + \dots + d_1 p Z + d_0 Z = d_0 W \quad (3)$$

For convenience, this equation is normalized with respect to a cutoff frequency,  $\omega_0$ , by use of the substitutions

$$\omega_0^n = \frac{d_0}{d_n} \quad (4a)$$

$$q_i = \frac{d_i}{d_n} \omega_0^{i-n} \quad (4b)$$

$$S = \frac{D}{\omega_0} \quad (4c)$$

Equation (3) then becomes

$$S^n Z + q_{n-1} S^{n-1} Z + \dots + q_1 S Z + Z = W \quad (5)$$

A block diagram of the filter represented by (5) is shown in Fig. 2-2.

No differentiator is used in the mechanization of the filter. The filter consists only of summing, integrating and coefficient units. The general availability of various derivatives of the output is indicated in the figure. For example, the first derivative of the output ( $SZ$ ) is simply the input to the last integrator to the right in the figure. Succeedingly higher derivatives are obtained as the inputs to the preceding integrators.

Returning to the basic problem, let such a linear filter which is denoted by the operator  $L(p)$ , replace the derivative computer in Fig. 2-1, and let the system input  $y$  be passed through an identical filter, as indicated in Fig. 2-3. The filter whose input is  $x$  produces an output which is denoted by  $x_c$ . Thus,

$$L(p)x = x_c \quad (6)$$

In addition, this filter has available from it the higher derivatives of  $x_c$ , namely  $px_c$ ,  $p^2x_c$ ,  $\dots$ ,  $p^nx_c$ . These derivatives of the filter output are related to the derivatives of the input as follows:

$$\begin{aligned} px_c &= pL(p)x = L(p)(px) \\ &\vdots \\ p^nx_c &= p^nL(p)x = L(p)(p^nx) \end{aligned} \quad (7)$$

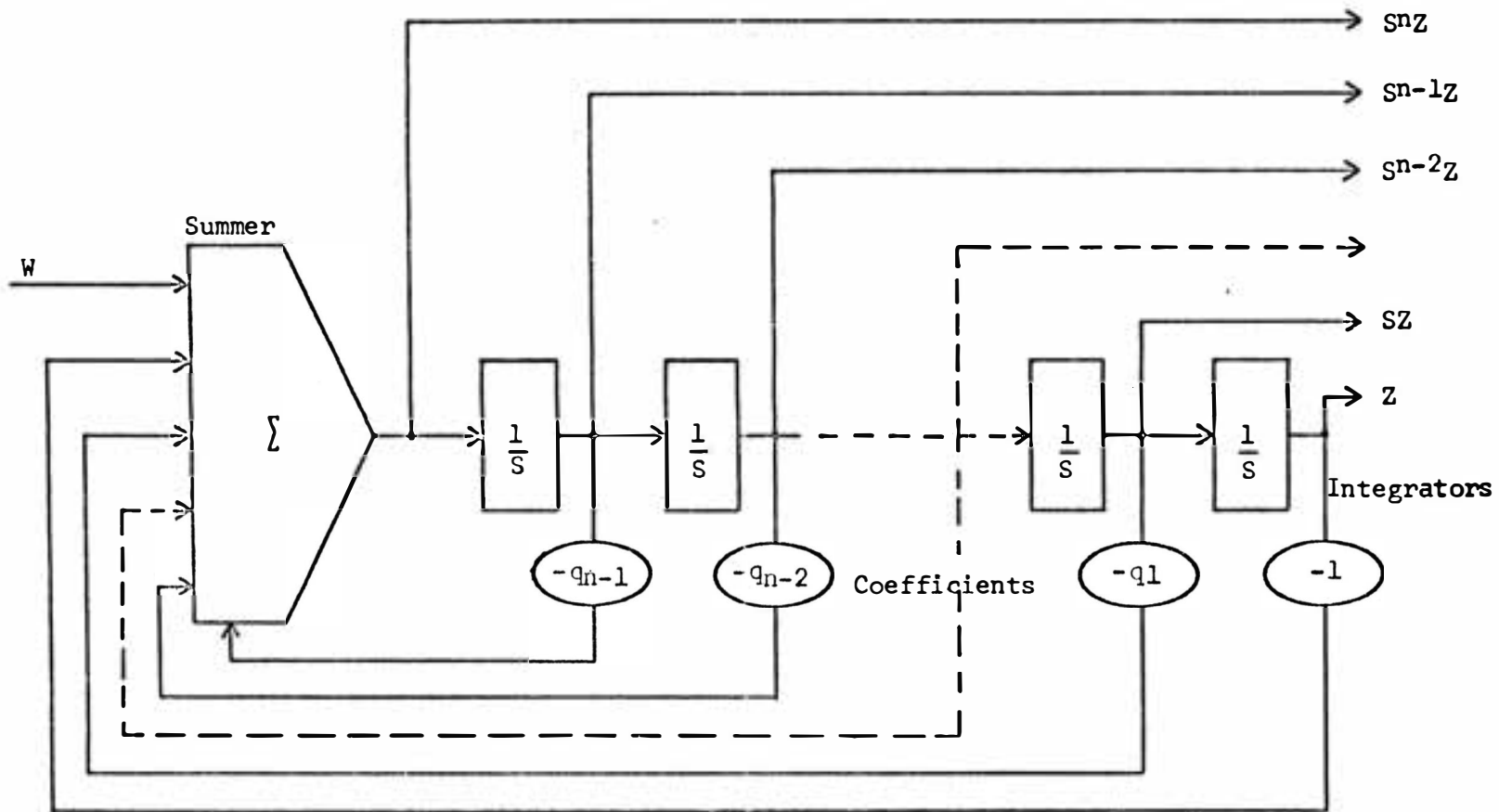


Fig. 2-2. Mechanization of a filter to provide derivatives of the output.

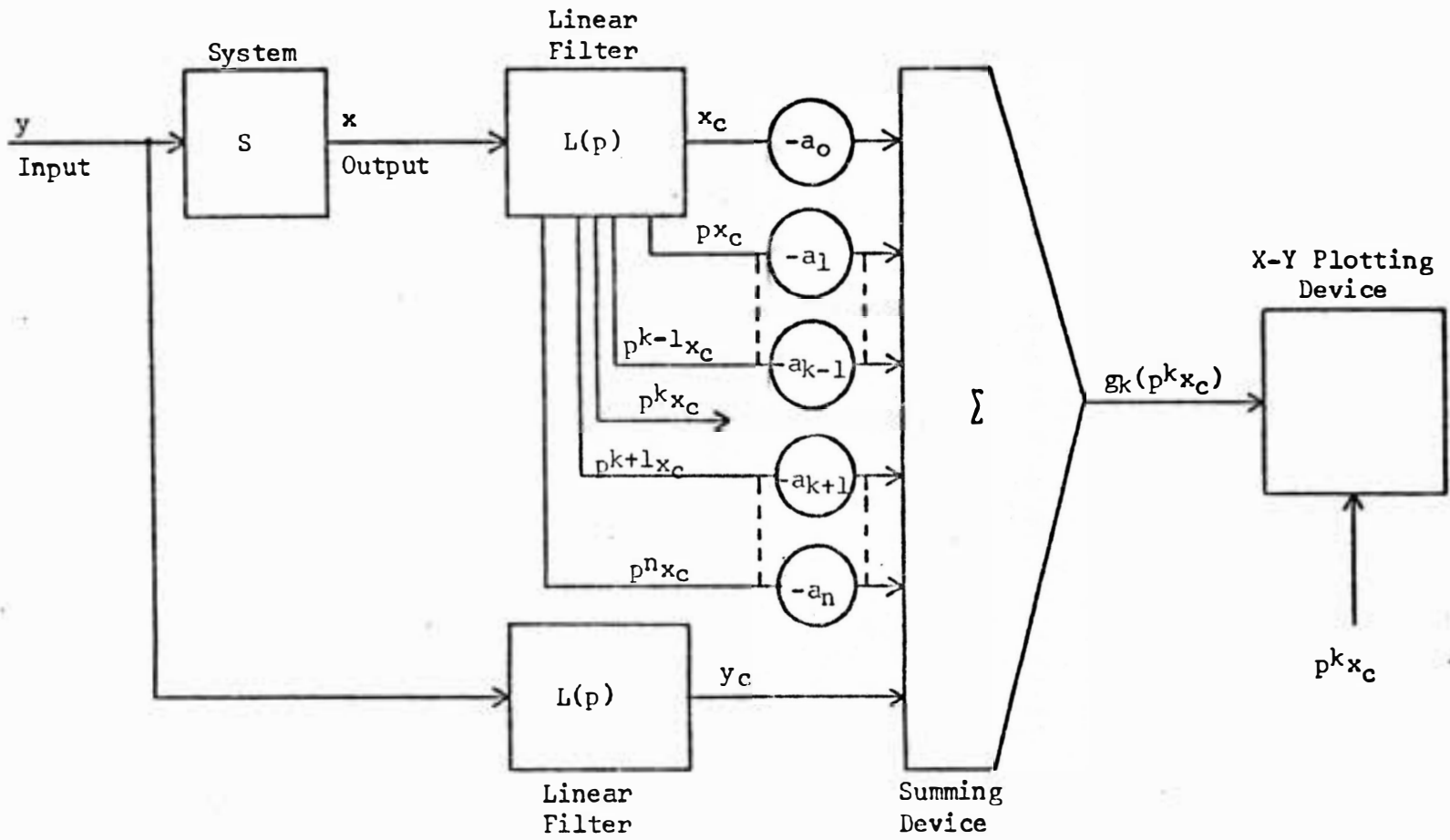


Fig. 2-3. Practical calculation of a nonlinear function.

The equivalence of  $p^n L(p)x$  and  $L(p)(p^n x)$  follows from the commutative property of the linear operators  $p^n$  and  $L(p)$ .

A similar operation on the system input  $y$  results in

$$L(p)y = y_c \quad (8)$$

The application of these two filters results in the computation of a quantity  $g_k(p^k x_c)$  which is plotted against  $p^k x_c$ . The quantity  $g_k(p^k x_c)$  is an approximation to the actual nonlinear function  $f_k(p^k x)$  and

$$g_k(p^k x_c) = y_c - (a_n p^n x_c + a_{n-1} p^{n-1} x_c + \dots + a_{k+1} p^{k+1} x_c + a_{k-1} p^{k-1} x_c + \dots + a_1 p x_c + a_0 x_c) \quad (9)$$

The right-hand side of this equation may also be obtained by operating on (2) with  $L(p)$ . Thus,

$$g_k(p^k x_c) = L(p)f_k(p^k x) \quad (10)$$

This expression gives the relationship between the calculated nonlinear function  $g_k(p^k x_c)$  and the actual nonlinear function  $f_k(p^k x)$ . An accurate determination of  $f_k(p^k x)$  can be made from the function  $g_k(p^k x_c)$  provided that both have the same form, or that

$$g_k(p^k x_c) = f_k(p^k x_c) \quad (11)$$

Substituting this relationship into (10) yields

$$f_k(p^k x_c) = L(p)f_k(p^k x), \quad (12)$$

and using

$$p^k x_c = L(p)p^k x \quad (13)$$

it follows that

$$f_k[L(p)p^k x] = L(p)f_k(p^k x). \quad (14)$$

In this last expression the calculated nonlinear quantity is equated to the actual nonlinear function which appears on the right. If  $f_k$  is

regarded as a nonlinear operator which operates on  $p^k x$ , the result of (14) is to require that the linear operator  $L(p)$  must commute with the nonlinear operator  $f_k$ . If this condition is met, the characteristic curve of the nonlinear element will be obtained by plotting  $g_k(p^k x_c)$  as a function of  $p^k x_c$  as indicated in Fig. 2-3.

As a consequence of (14) it is necessary to determine some linear operator  $L(p)$  which commutes with the variety of nonlinear operators encountered in physical systems. According to Kohr, one such operator is the dead time or transport lag operator (or filter)  $T_L(p)$ . A heuristic argument for the suitability of this operator is as follows: the result of passing a time function through a nonlinear operator and then passing this result through a transport lag filter is exactly the same when the nonlinear operator and the transport lag filter are interchanged. The commutability of this transport lag filter with various nonlinear operators has been verified experimentally.

A sinusoidal input was applied to the linear filter and its output was fed into the nonlinearity. A plot of the final output versus sinusoidal input was obtained on the x-y plotter. A similar procedure was repeated after interchanging the linear filter and the nonlinearity. If the two plots were identical, then the linear filter selected was commutable with that nonlinearity.

Three distinct problems occur in the application of differential equations and operational mathematics to physical systems. These problems have been named the analysis, instrument, and synthesis problems<sup>9</sup>.

The analysis problem is to find the output, given the input and the mathematical description of the system.

The instrument problem is to find the input, given the output and the mathematical description of the system.

The synthesis problem is to determine the mathematical description of the system, given the input and the desired output.

It is clear that the synthesis problem is intimately related to engineering design. Typical inputs are often known and the desired output may be subject to specification.

Thus our remaining problem of determining a mathematical form for a linear filter  $L(p)$  which will provide the required derivatives of output as well as output, falls under the synthesis category.

The linear filter will also act as a transport lag device. A system which produces a transport lag has a frequency response that exhibits a constant amplitude ratio of unity and a phase shift that varies linearly with frequency for all frequencies. No filter composed of a finite number of lumped parameter elements can produce exactly this response. Therefore, an approximation to the transport lag must be accepted and the problem is reduced to selecting the coefficients of (5) which provide a transport lag approximation.

Hence Kohr investigated the following four sets of coefficients.

1. Minimum attenuation (Butterworth) coefficients.
2. Linear phase (Bessel) coefficients.
3. Padé coefficients.
4. ITAE (Integral of Time-multiplied Absolute value of Error)

coefficients.

For a given cutoff frequency  $\omega_0$ , as defined in (4), the Butterworth coefficients provide a maximally-flat amplitude characteristic and a phase characteristic which is linear only for frequencies  $\omega$  such that  $\omega \ll \omega_0$ . The converse is true for Bessel coefficients. The Padé coefficient for third- and fourth-order approximations produce undesirable resonances in the amplitude response. Padé approximations for fifth and higher orders also represent unstable systems and are consequently unusable. The ITAE coefficients provide an amplitude response which is flatter than that of Bessel coefficients and a phase response which is more linear than provided by the Butterworth coefficients. The ITAE coefficients thus represent a reasonable compromise between the Butterworth and Bessel coefficients. The function  $I = \int_0^{\infty} t|e|dt$  is known as the integral of time-multiplied absolute value of error (ITAE) criterion. Also, Graham and Lathrop<sup>9</sup> demonstrated the clear superiority of the filters with ITAE coefficients over binomial and Butterworth filters. Filters with ITAE coefficients have faster transient response than binomial filters and are less oscillatory than those of the Butterworth filters.

According to Graham and Lathrop<sup>9</sup>, the ITAE criterion is selective and easy to mechanize on an analog computer. If analog computation is employed in the study of linear or nonlinear systems for which no standard forms are available, the ITAE criterion may still be used as a unitary figure of merit for the rapid evaluation of a large number of filter parameters.



The ITAE coefficients used in this study are those which represent zero-displacement error systems. These coefficients have been established for systems up to eighth-order by Graham and Lathrop and are reproduced in the normalized form of (5) in Table 1. Standard forms can provide a quick and easy method for the synthesis of optimum dynamic response in a variety of applications.

The transport lag filter required to mechanize the calculation (9) may be selected from Table 1. It is necessary only to establish the cutoff frequency of the filter as defined by (4a) and the order of the filter. In order to provide a substantial attenuation of high frequency noise, it is usually desirable to select a filter whose order is greater than the order of the system under consideration.

Once the filter is chosen, the identification system is complete. The next step is to excite the system with a periodic input of low frequency. There is usually an upper limit on the input frequency that should not be exceeded if the nonlinear function is to be accurately determined. The limit depends upon the character of the nonlinear element and also the cutoff frequency of the transport lag filter. The accuracy of the identification of the nonlinearity also depends upon knowledge of the exact values of the coefficients of all the linear terms in (9).

Up to now, the identification process has been discussed based on the assumption that all the linear coefficients, except the nonlinear coefficient to be identified, are known. While prior knowledge of the linear coefficients is desirable, since it simplifies the identification

process, it is not always required. If the linear coefficients are not known beforehand, they can also be determined.

Assume that the system is of the form of (1) and that the differential equation assumed to represent the system is of the form

$$b_n p^n x_c + b_{n-1} p^{n-1} x_c + \dots + g_k(p^k x_c) + \dots + b_1 p x_c + b_0 x_c = y_c \quad (15)$$

In this situation, (10) is not satisfied and an error equation may be established as

$$g_k(p^k x_c) - L(p)f_k(p^k x) = (a_n - b_n)p^n x_c + \dots + (a_{k+1} - b_{k+1})p^{k+1} x_c + (a_{k-1} - b_{k-1})p^{k-1} x_c + \dots + (a_1 - b_1)p x_c + (a_0 - b_0)x_c. \quad (16)$$

The right-hand side of this equation may be seen as the difference between the calculated and actual nonlinear functions. When the right-hand side approaches zero, the calculated function approaches the actual nonlinear function.

In linear systems, a mismatch between the actual system coefficients and the coefficients in the assumed differential equation results in the plot of  $g_k(p^k x_c)$  vs  $p^k x_c$  becoming an ellipse. The plot will become a straight line for the correct coefficients. A nulling procedure may be used to determine the unknown coefficients. This procedure consists of exciting the system with a sinusoidal input of an arbitrary frequency  $\omega_1$ , and then adjusting the  $b_0$  coefficient until the ellipse is reduced as nearly as possible to a straight line. The system is then excited at some arbitrarily higher sinusoidal frequency  $\omega_2$ , and then  $b_1$  is adjusted in this same manner. The procedure is

continued, increasing the frequency each time, until all the coefficients have been adjusted. The entire procedure is then repeated from the beginning and is continued until all the coefficients take on unchanging values. All the frequencies  $\omega_1, \omega_2, \dots, \omega_n$ , used in this procedure should be less than one-tenth of the cutoff frequency  $\omega_0$  selected for the linear filter.

The same procedure may also be applied to nonlinear systems. In nonlinear systems, according to Kohr, a mismatch between system coefficients and those in the assumed equation results in the plot of  $g_k(p^k x_c)$  vs  $p^k x_c$  becoming a closed curve which should enclose the actual nonlinear function. Kohr also states that the coefficients in the assumed equation might be closely approximated to actual coefficients by adjusting each coefficient so that the area inside the closed curve is reduced to a minimum.

While the criteria of minimum area inside the closed curve to determine the unknown linear coefficients applies to systems containing single-valued nonlinearities, it certainly does not apply to systems containing double-valued nonlinearities. This statement will be substantiated in the subsequent chapters with experimental results obtained by the author.

So far it has been assumed that the system contains only one nonlinear element. In a system which contains more than a single nonlinear coefficient, an iteration procedure like that used for unknown linear coefficients may be used to determine the nonlinear elements. For example, assume that the actual system contains two

nonlinear elements that may be represented by  $f_j(p^j x)$  and  $f_k(p^k x)$ . The system equation may then be written as

$$a_n p^n x + a_{n-1} p^{n-1} x + \dots + f_j(p^j x) + \dots + f_k(p^k x) + \dots + a_1 p x + a_0 x = y. \quad (17)$$

The two nonlinear functions are determined by the use of two equations. In the first equation the calculated nonlinear function  $g_j(p^j x_c)$  is assumed initially to be linear and of the form  $a_j p^j x_c$ , while in the second equation the nonlinear function  $g_k(p^k x_c)$  is allowed to retain its nonlinear form. The two equations are

$$g_k(p^k x_c) = y_c - (a_n p^n x_c + a_{n-1} p^{n-1} x_c + \dots + a_j p^j x_c + \dots + a_{k+1} p^{k+1} x_c + a_{k-1} p^{k-1} x_c + \dots + a_1 p x_c + a_0 x_c) \quad (18)$$

and,

$$g_j(p^j x_c) = y_c - (a_n p^n x_c + a_{n-1} p^{n-1} x_c + \dots + a_{j+1} p^{j+1} x_c + a_{j-1} p^{j-1} x_c + \dots + g_k(p^k x_c) + \dots + a_1 p x_c + a_0 x_c). \quad (19)$$

Equation (18) is then solved for  $g_k(p^k x_c)$  and (19) is solved for  $g_j(p^j x_c)$ . The solution proceeds iteratively as follows:

- 1) A first value of the function  $g_k(p^k x_c)$  is determined from (18) by adjusting the coefficient  $a_j$  for the minimum enclosed area in the plot of  $g_k(p^k x_c)$  vs  $p^k x_c$ .
- 2) The function  $g_k(p^k x_c)$  thus obtained is inserted into (19) which permits a first determination of  $g_j(p^j x_c)$ .
- 3) The function  $g_j(p^j x_c)$  thus obtained is inserted into (18) in place of the quantity  $a_j p^j x_c$ . A new functional form of

$g_k(p^k x_c)$  is then found.

- 4) Further iterations are performed until  $g_k(p^k x_c)$  and  $g_j(p^j x_c)$  take on unchanging forms. The successive nonlinear functions obtained for  $g_k(p^k x_c)$  must be simulated for each new approximation of  $g_j(p^j x_c)$  and vice versa. The time required to make the calculations is materially increased when two or more nonlinear functions must be determined, due to the time required to mechanize the newly discovered nonlinear function for the next calculations.

CHAPTER III  
APPLICATION OF KOHR'S METHOD TO SYSTEMS  
CONTAINING SINGLE-VALUED NONLINEARITIES

Kohr's method was applied to first-order systems containing single-valued nonlinearities and the experimental results obtained are given in this chapter. Three different first-order systems containing limiting type, dead zone type, and relay type nonlinearities respectively, were identified.

A. Limiting element in a first-order system (Fig. 3-1).

The system used in the experiment was of the form,

$$a_1 p x + f_0(x) = y \quad (20)$$

where  $f_0(x)$  is the nonlinear element; in this case saturating or limiting type of element, and the linear coefficient

$$a_1 = 1$$

The simulation scheme given in Appendix A (Fig. A-1) was used in the identification of the systems. The simulation diagram for the limiting type nonlinearity is shown in Fig. B-1.

Figures 3-2, 3-3, 3-4, and 3-5 show the calculation of the nonlinear function for input frequencies 0.75, 0.5, 0.25 and 0.1 rad/sec, respectively. The correct linear coefficient (1.0) was used in the calculation to illustrate the error in the identification of the nonlinear function at higher than one-tenth of the cutoff frequency. The error at higher frequencies is due to higher harmonic frequencies, generated by the nonlinear element, which exceed the bandwidth of the linear filter. A

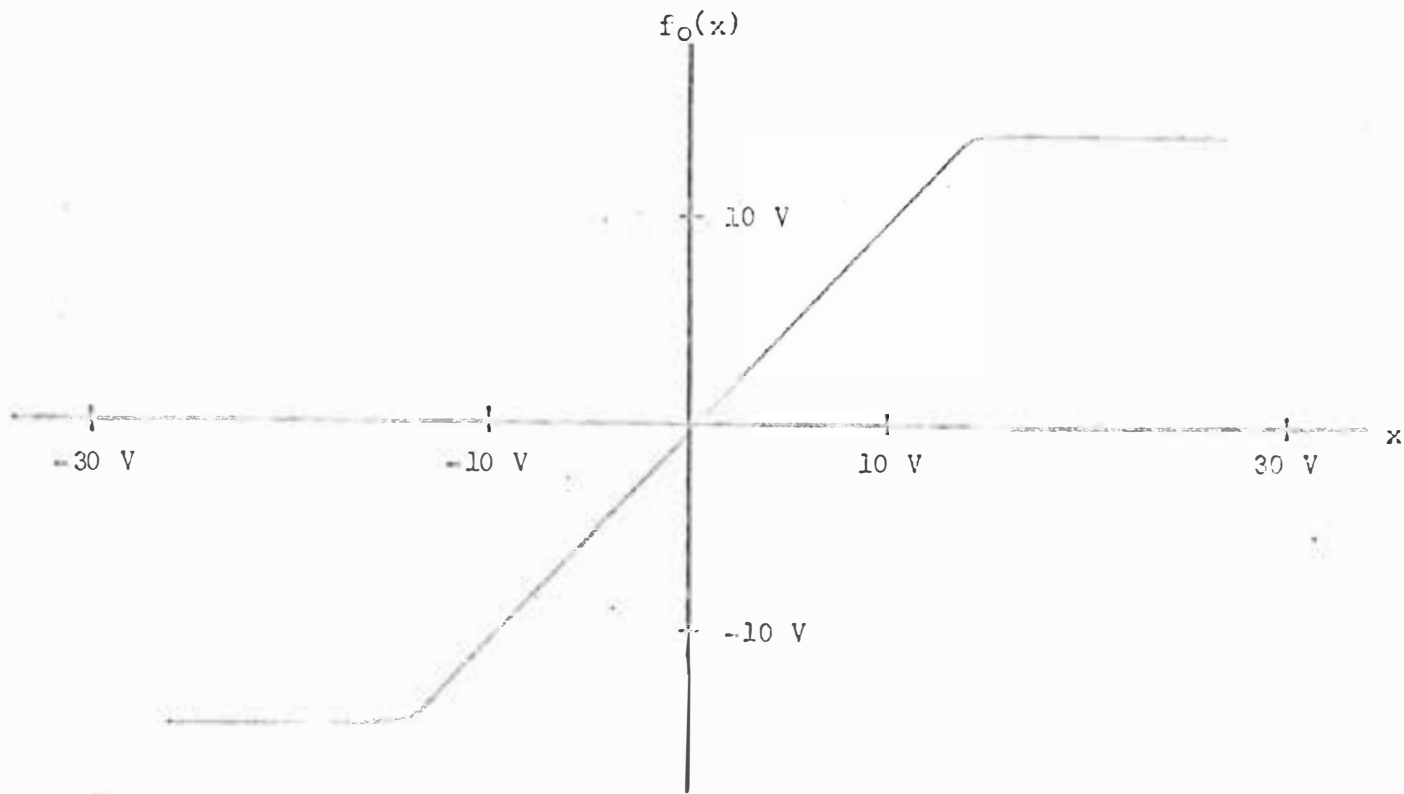


Fig. 3-1. Simulated limiting type nonlinearity.

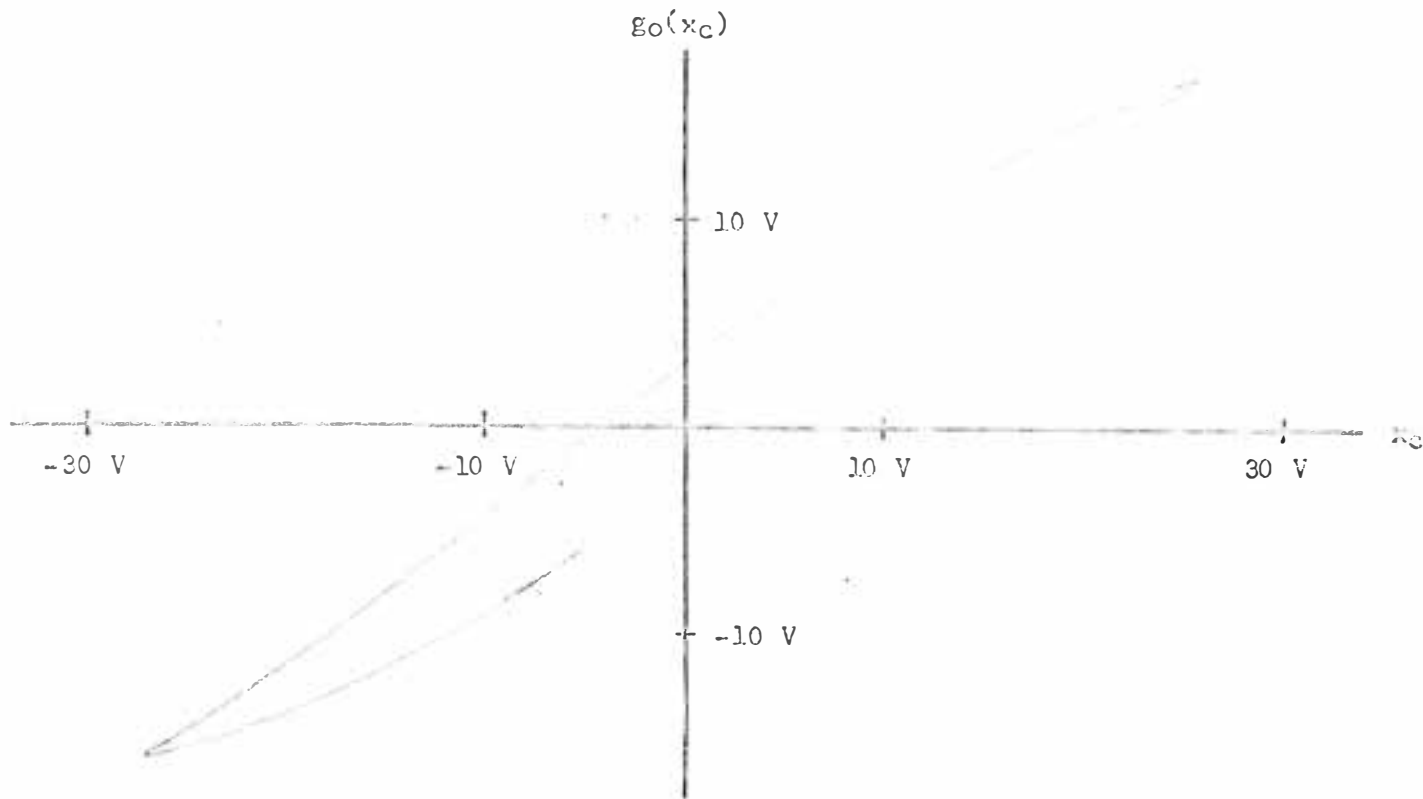


Fig. 3-2. Calculated nonlinear function (limiting) for  $\omega = 0.75$  rad/sec, and  $a_1 = 1.0$ .



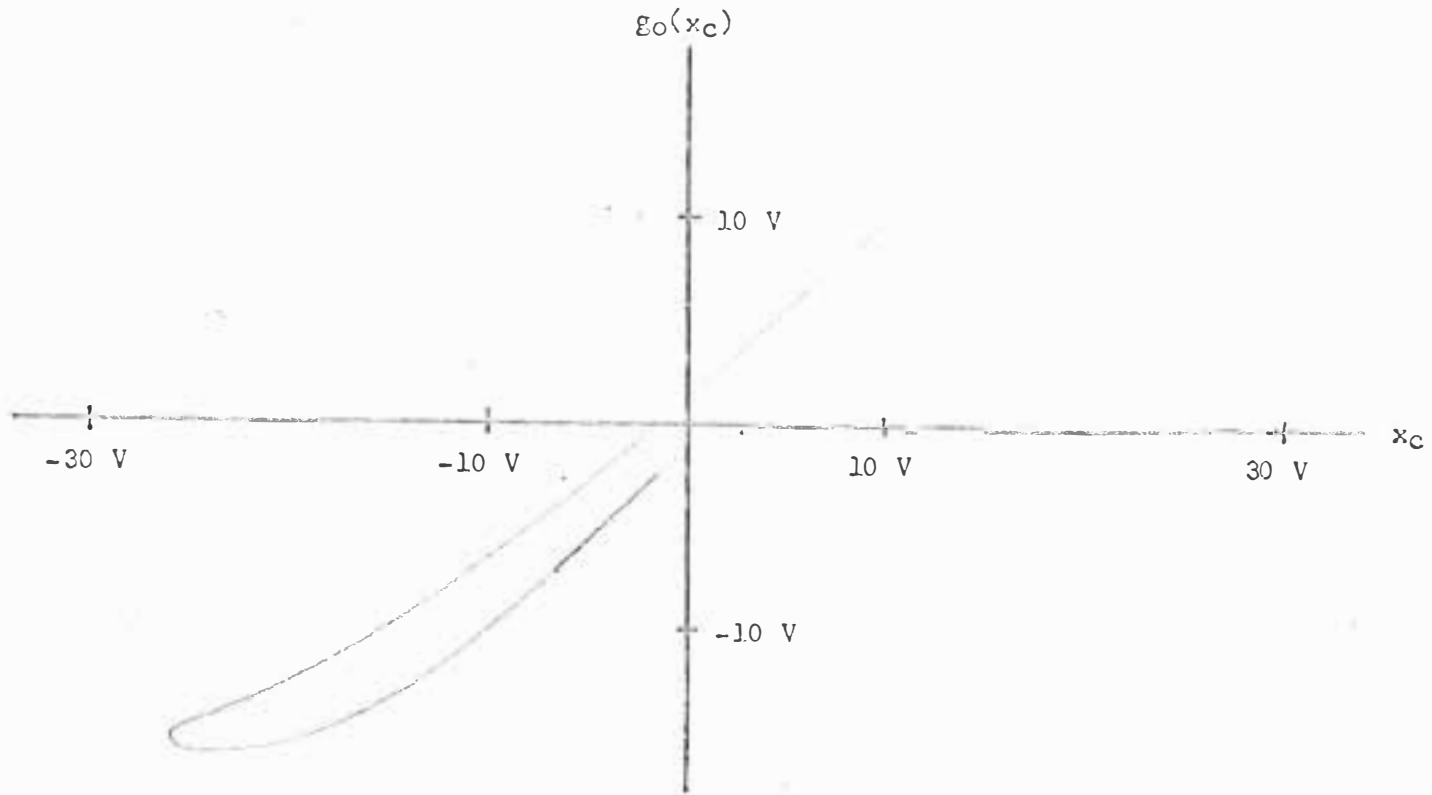


Fig. 3-3. Calculated nonlinear function (limiting) for  $\omega = 0.5$  rad/sec, and  $a_1 = 1.0$ .

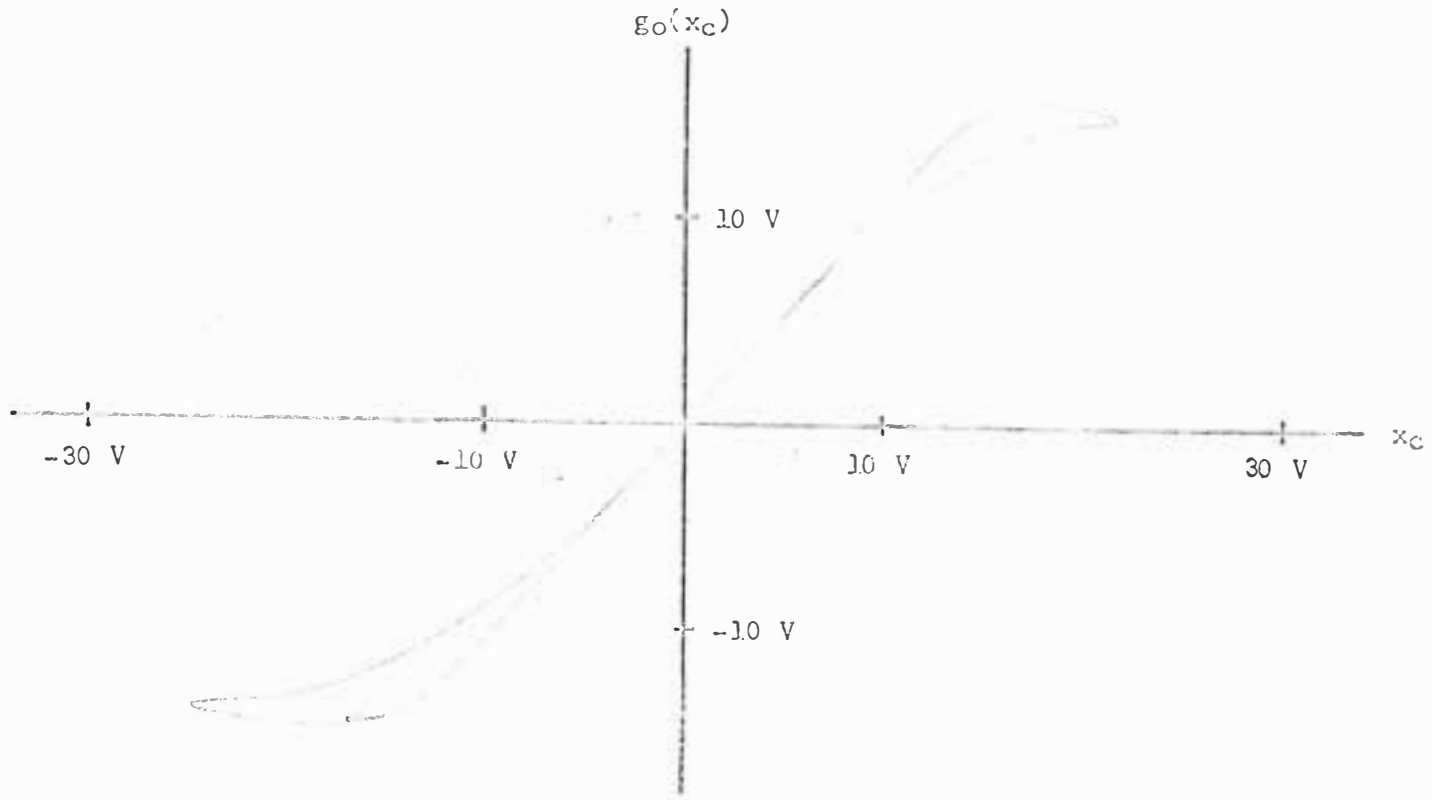


Fig. 3-4. Calculated nonlinear function (limiting) for  $\omega = 0.25 \text{ rad/sec}$ , and  $a_1 = 1.0$ .

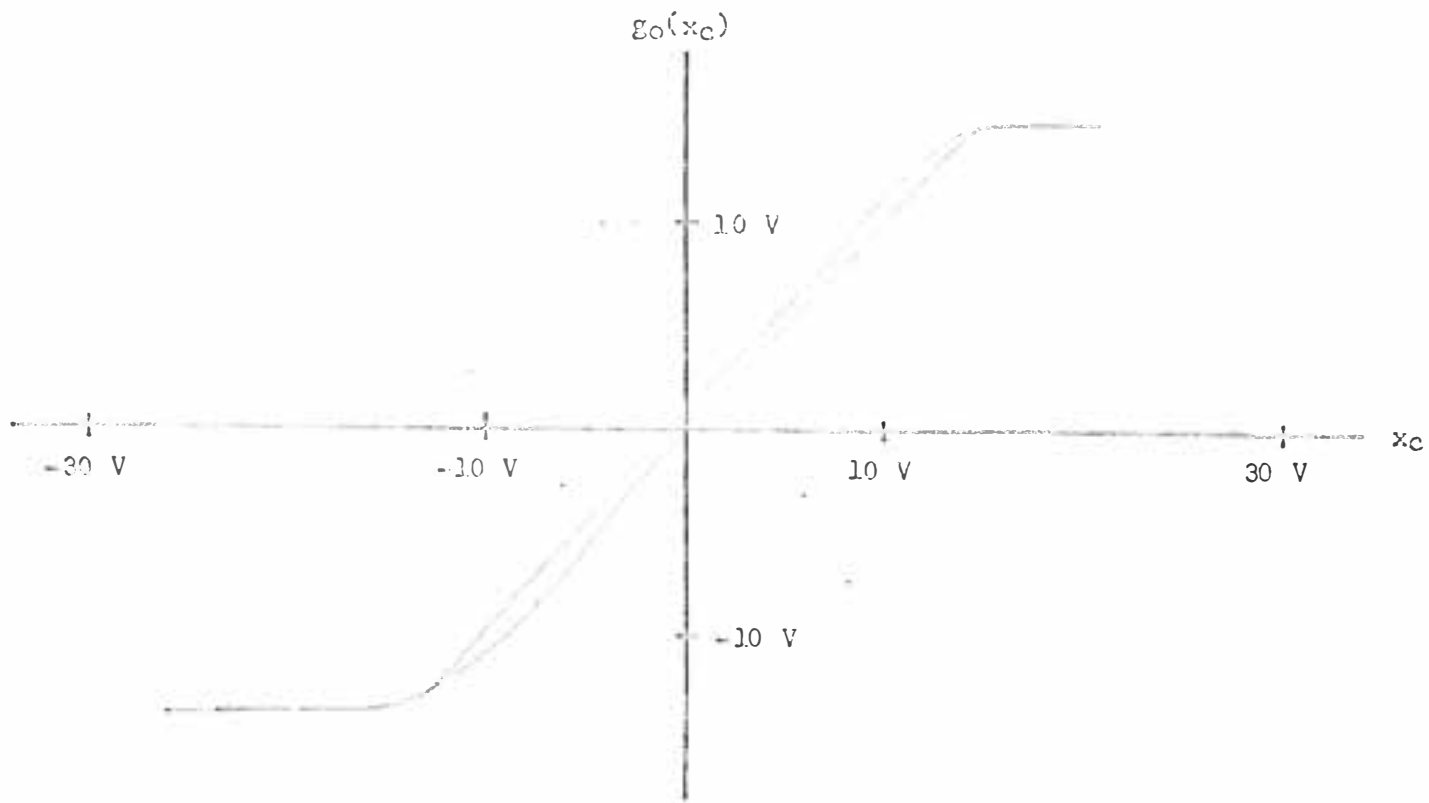


Fig. 3-5. Calculated nonlinear function (limiting) for  $\omega = 0.1$  rad/sec, and  $a_1 = 1.0$ .

second-order linear filter with a cutoff frequency of 1 rad/sec was used. An input frequency of 0.1 rad/sec gave satisfactory results and hence was used throughout the identification of various nonlinearities.

The unknown linear coefficient  $a_1$  was found by adjusting the coefficient  $a_1$  such that the area enclosed by the plot  $g_o(x_c)$  vs  $x_c$  is minimum. The plots corresponding to various values of  $a_1$  (viz., 1.0, 1.25, 1.5, 0.75 and 0.5) and  $\omega = 0.1$  rad/sec are shown in Figures 3-5 through 3-9. It is evident from the plots that the area enclosed is minimum when  $a_1 = 1.0$ . The area enclosed by the plot is minimum for the correct coefficient, i.e., 1.0. Also the area enclosed by the plot increases when the adjusted value of the linear coefficient is higher or lower than the correct value. Hence the calculated value of the linear coefficient is 1.0. The plot  $g_o(x_c)$  vs  $x_c$ , for  $a_1 = 1.0$ , at an input frequency of 0.1 rad/sec, represents the calculated nonlinear function (Fig. 3-5). The calculated nonlinear function closely approximates the actual nonlinear function (Fig. 3-1).

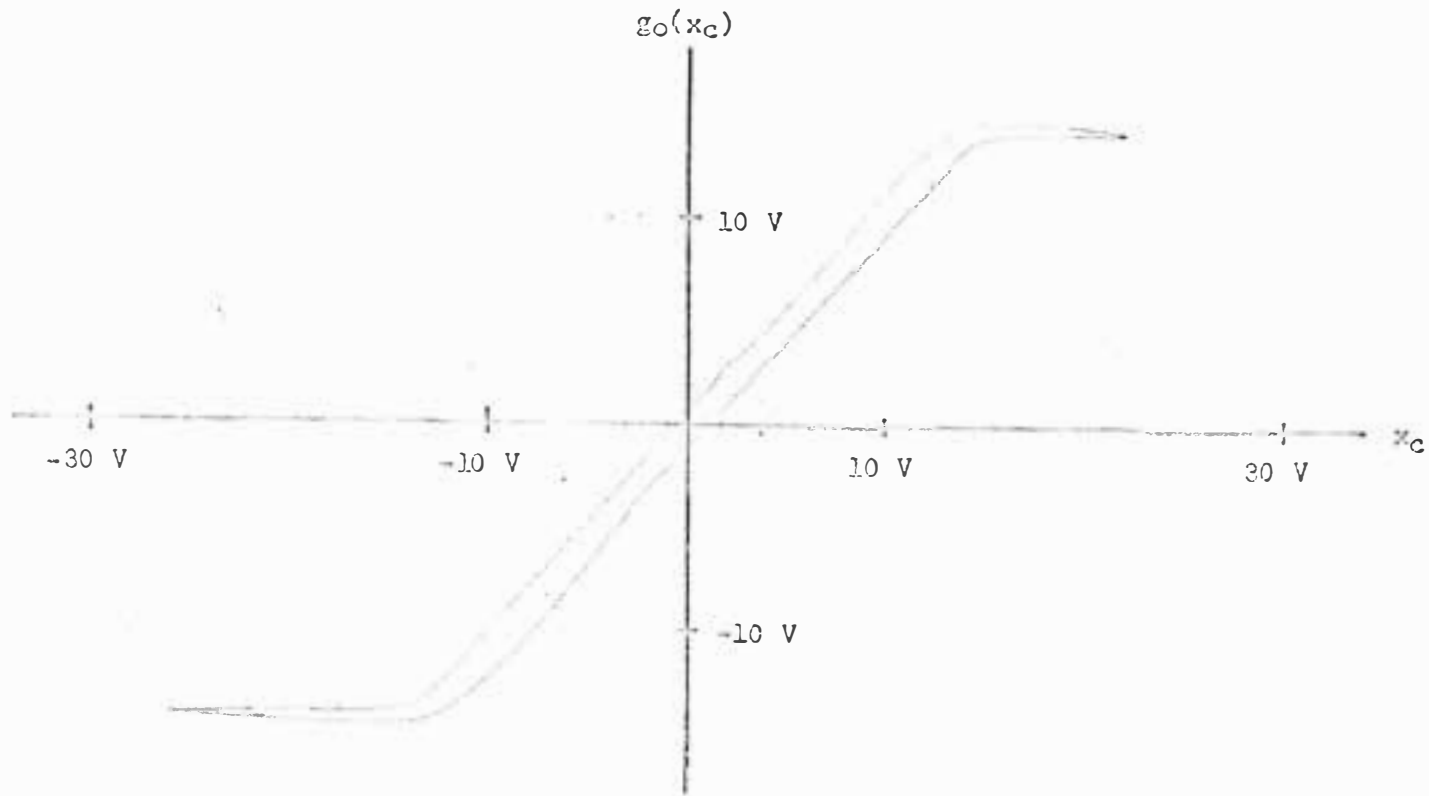


Fig. 3-6. Calculated nonlinear function (limiting) for  $\omega = 0.1$  rad/sec, and  $a_1 = 1.25$ .

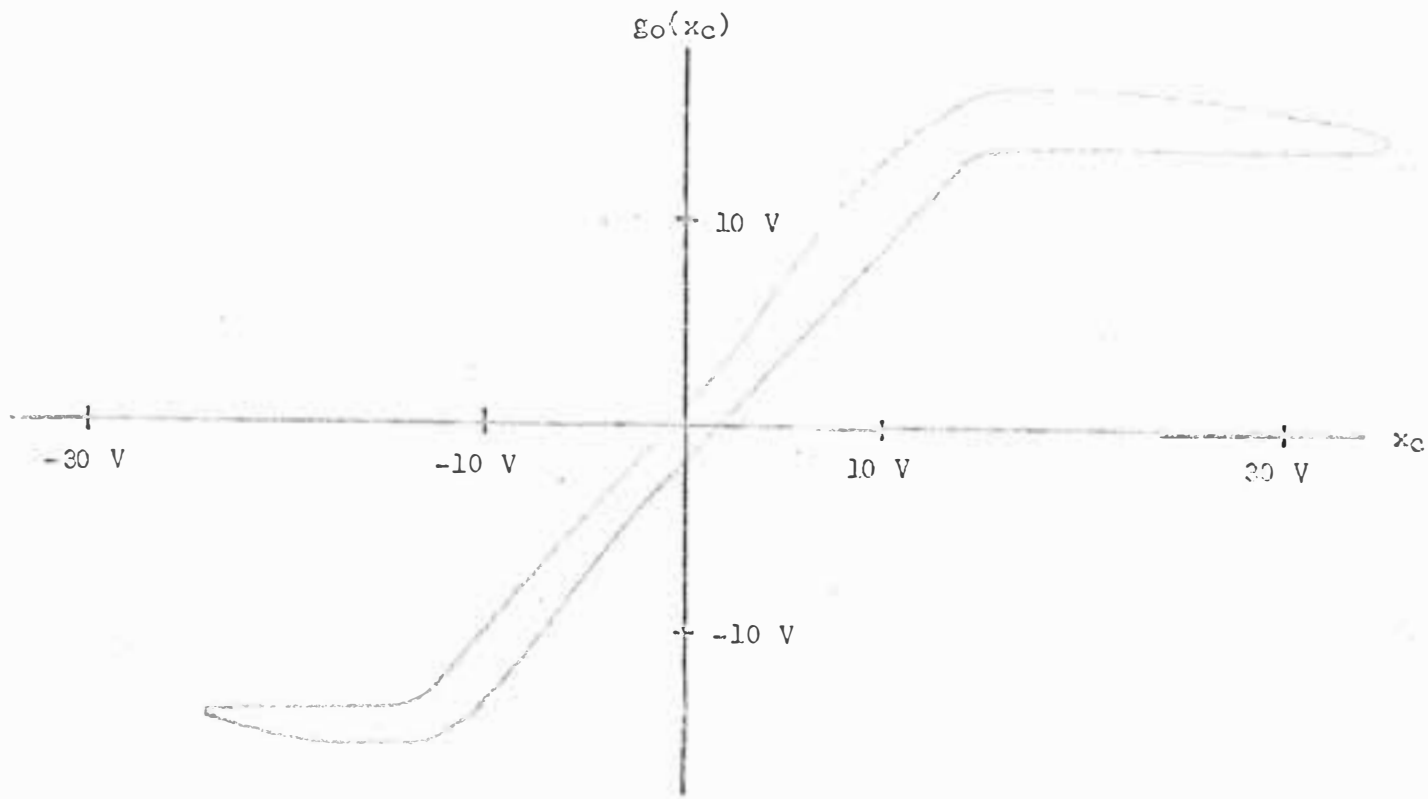


Fig. 3-7. Calculated nonlinear function (limiting) for  $\omega = 0.1$  rad/sec, and  $a_1 = 1.5$ .

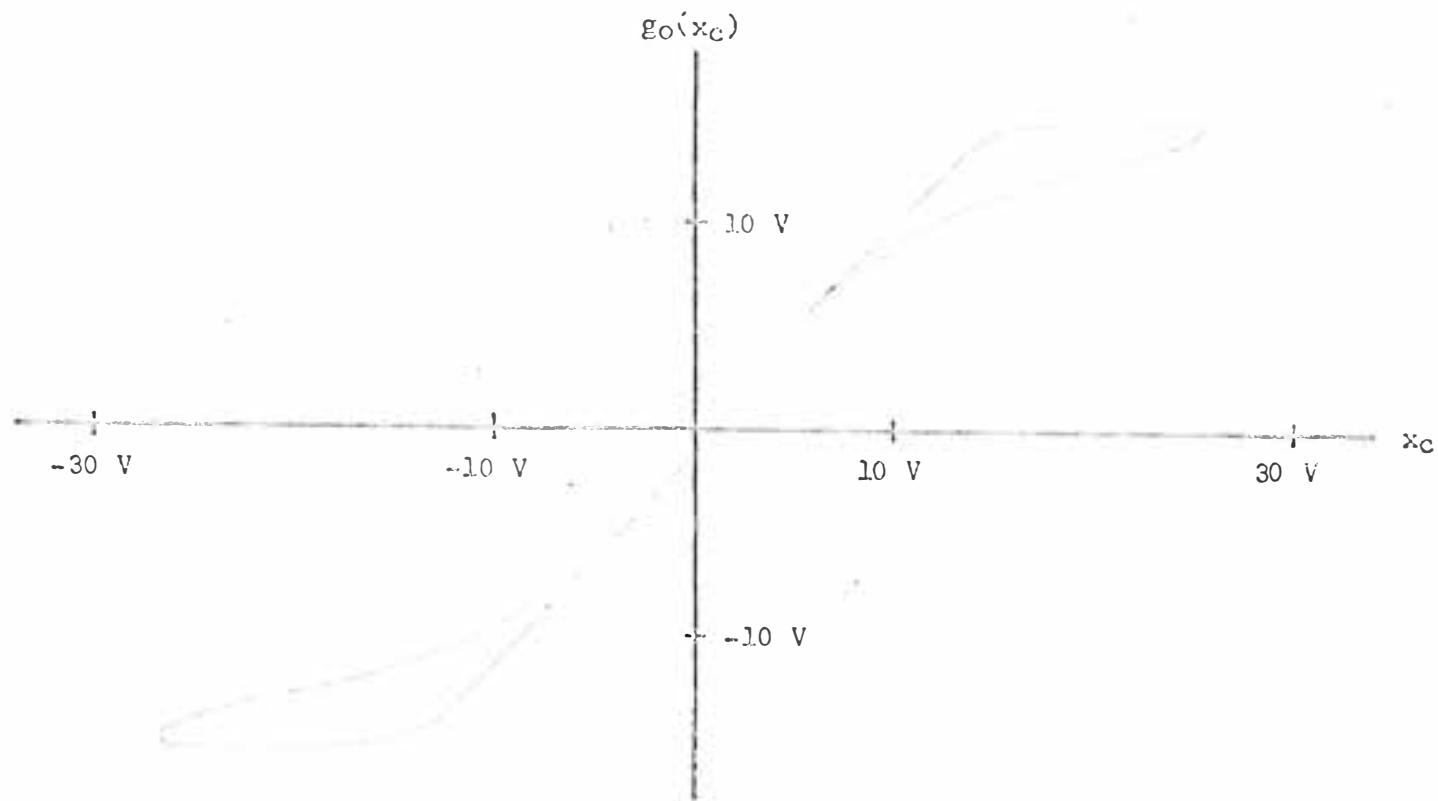


Fig. 3-8. Calculated nonlinear function (limiting) for  $\omega = 0.1$  rad/sec, and  $a_1 = 0.75$ .

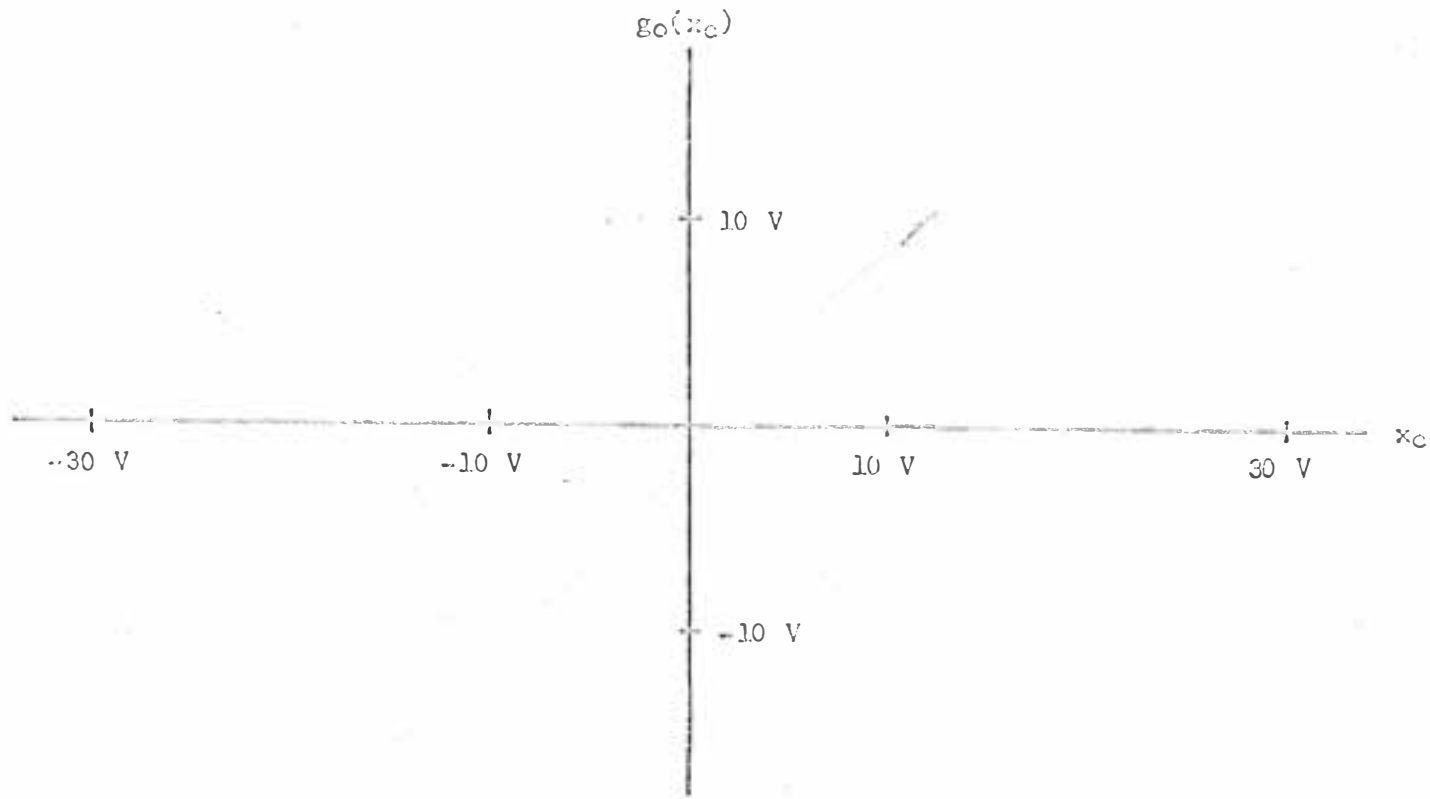


Fig. 3-9. Calculated nonlinear function (limiting) for  $\omega = 0.1$  rad/sec, and  $a_1 = 0.5$ .



B. Dead zone element in a first-order system.

The system was of the form given by (20) with  $f_0(x)$  denoting the dead zone element and  $a_1 = 1.0$ . The simulation of the nonlinearity is shown in Fig. B-2 and the actual nonlinear function is shown in Fig. 3-10. The  $g_0(x_c)$  vs  $x_c$  plots for  $a_1 = 1.0, 1.25, 1.5, 0.75,$  and  $0.5$  at an input frequency of  $0.1$  rad/sec are shown in Figures 3-11, 3-12, 3-13, 3-14, and 3-15, respectively. The area enclosed by the plot is minimum when  $a_1 = 1.0$ , and hence Fig. 3-11 represents the calculated nonlinear function and is nearly the same as the actual nonlinear function.

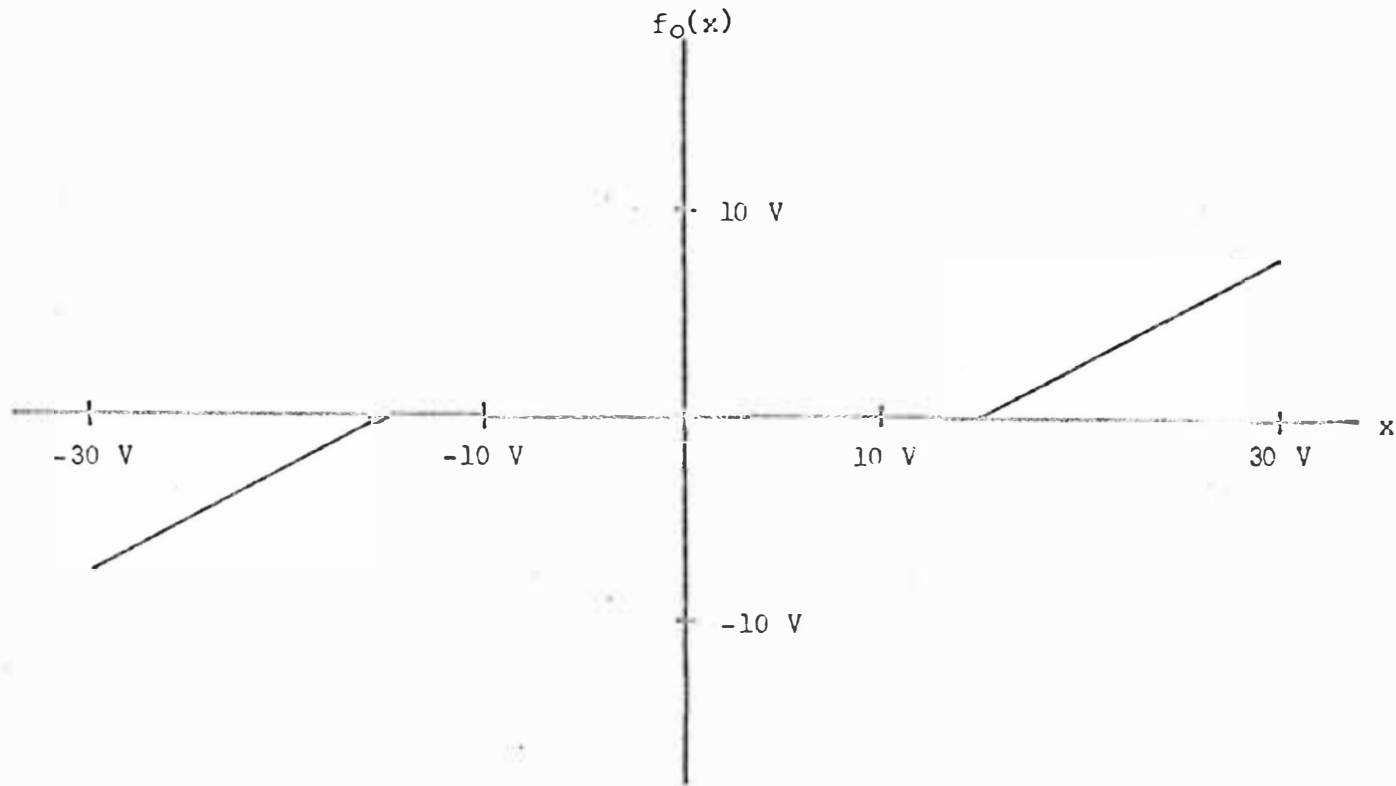


Fig. 3-10. Simulated dead zone type nonlinearity.

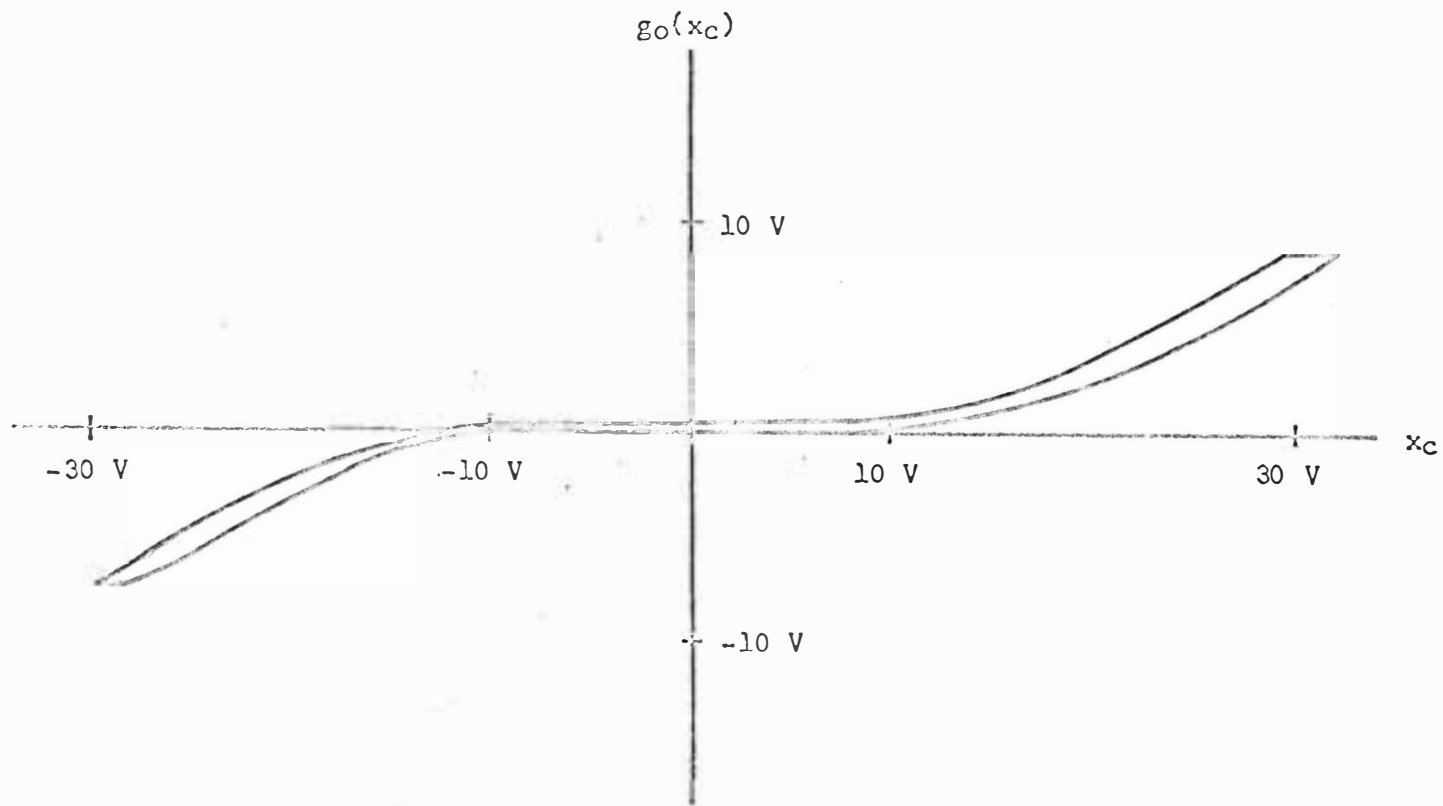


Fig. 3-11. Calculated nonlinear function (dead zone) for  $\omega = 0.1$  rad/sec, and  $a_1 = 1.0$ .

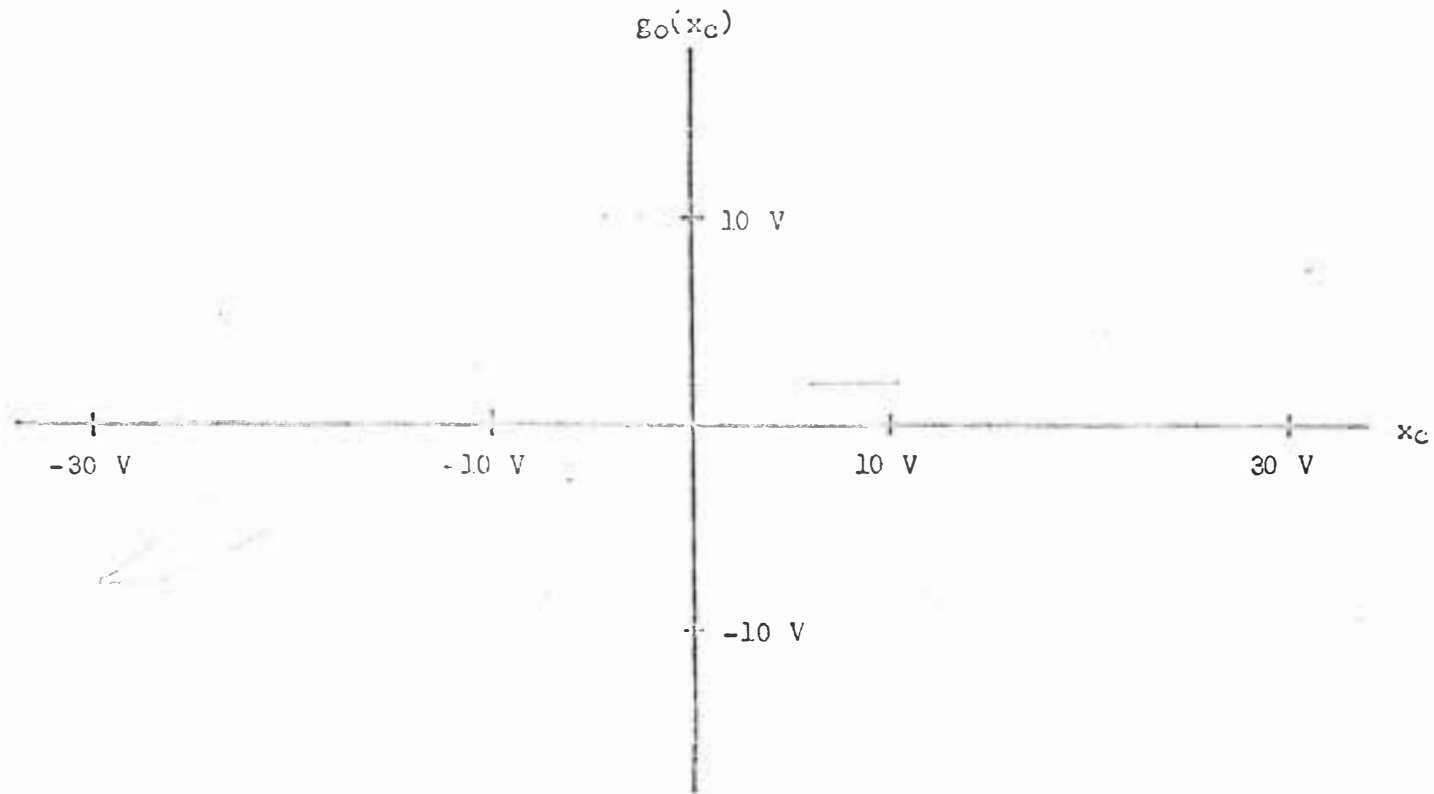


Fig. 3-12. Calculated nonlinear function (dead zone) for  $\omega = 0.1\text{ rad/sec}$ , and  $a_1 = 1.25$ .

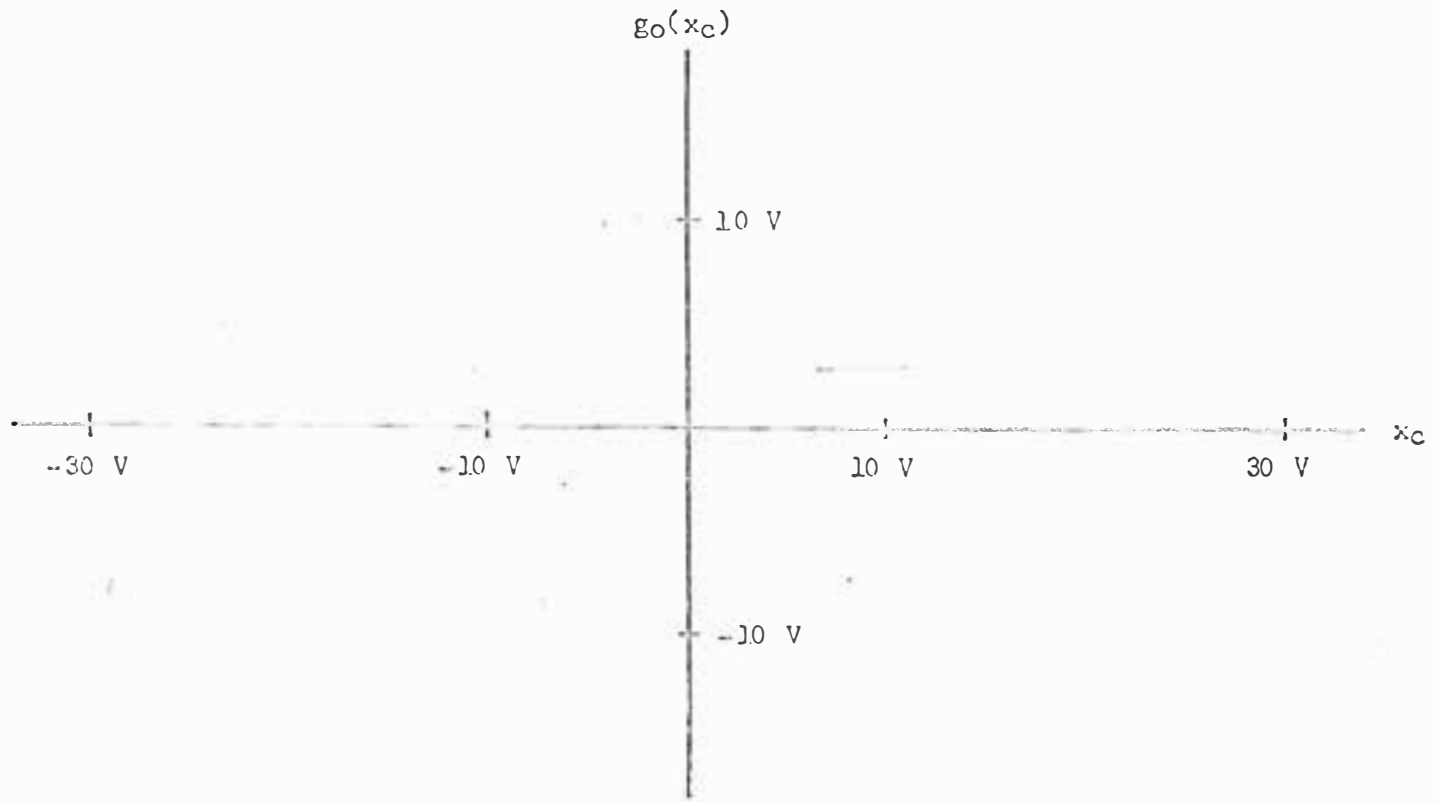


Fig. 3-13. Calculated nonlinear function (dead zone) for  $\omega = 0.1$  rad/sec, and  $a_1 = 1.5$ .

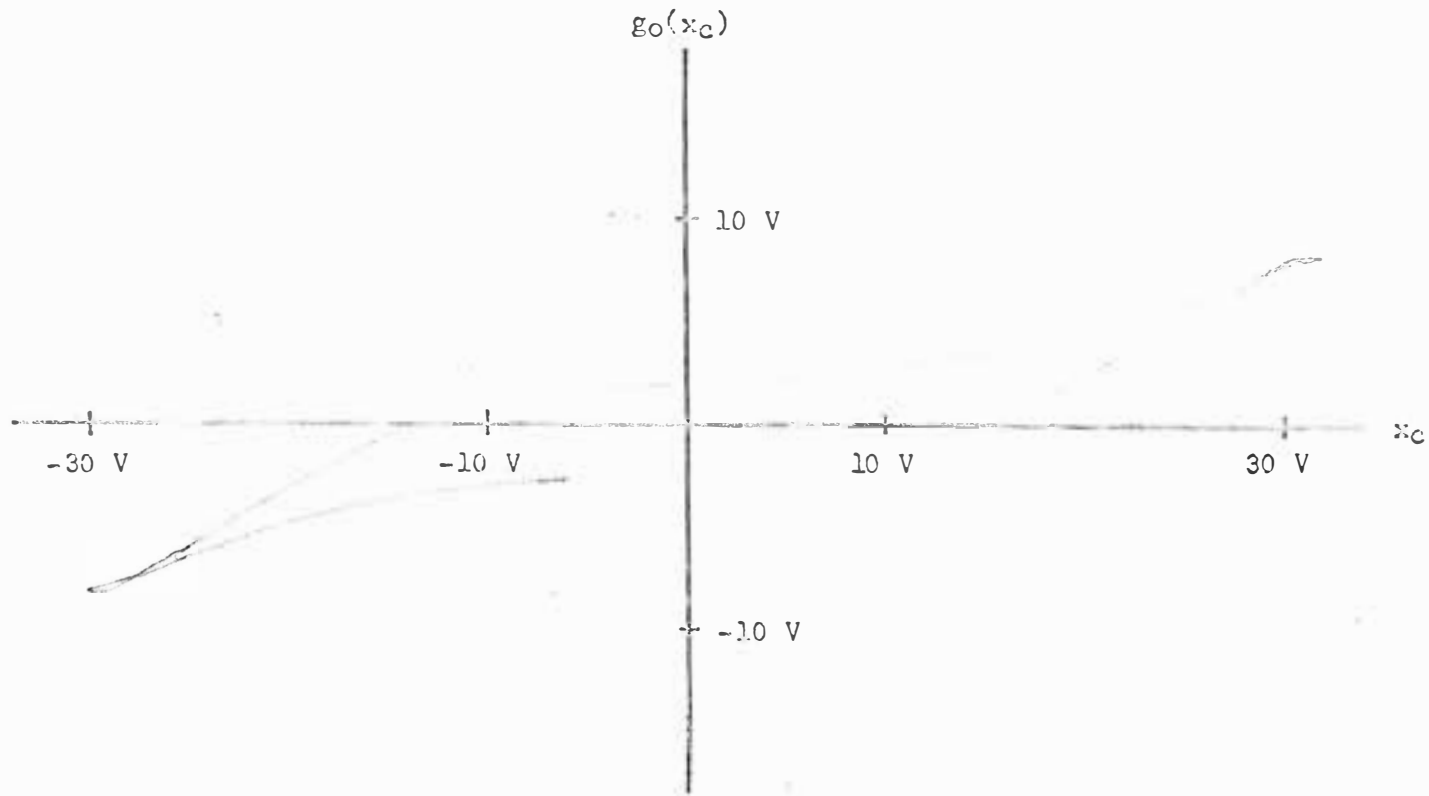


Fig. 3-14. Calculated nonlinear function (dead zone) for  $\omega = 0.1$  rad/sec, and  $a_1 = 0.75$ .

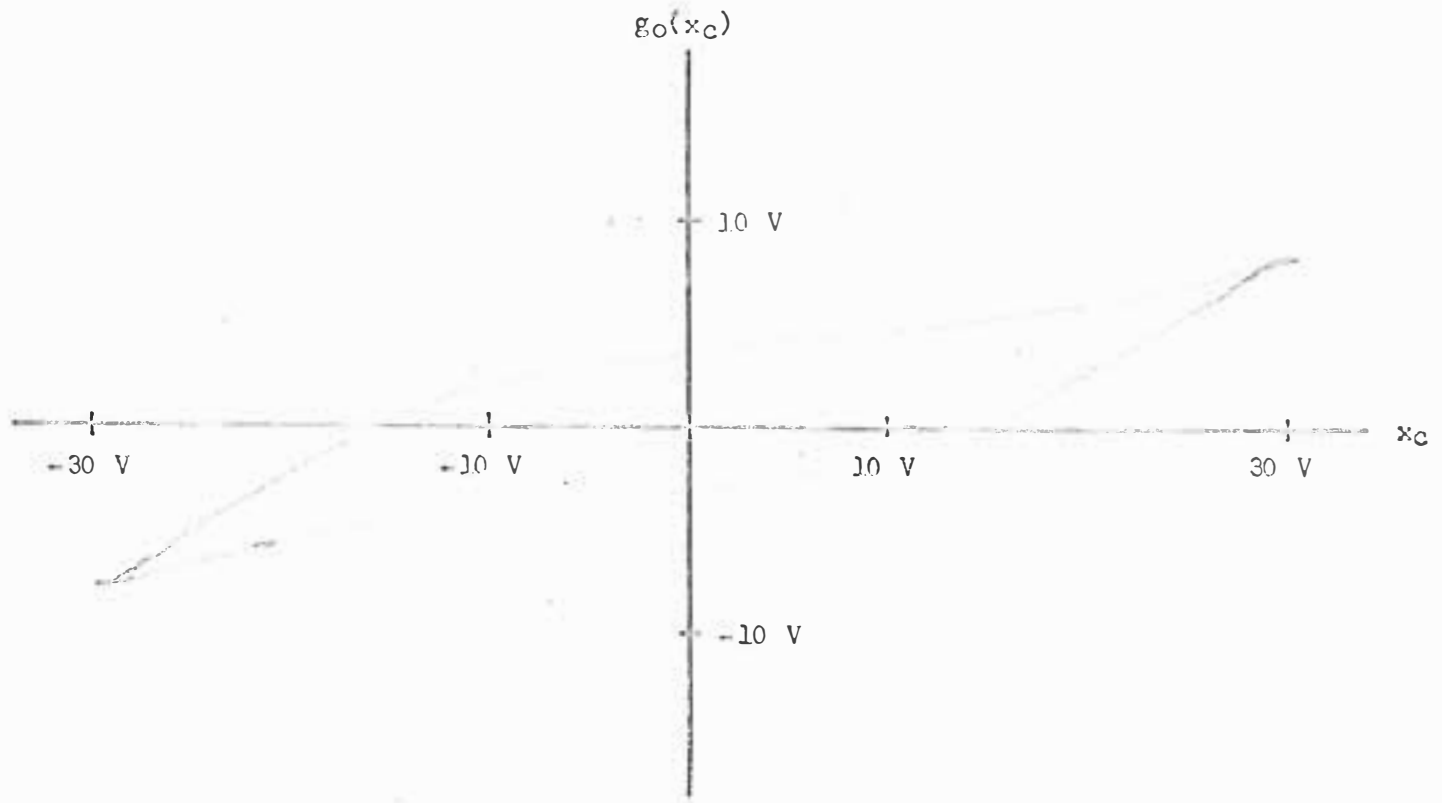


Fig. 3-15. Calculated nonlinear function (dead zone) for  $\omega = 0.1$  rad/sec, and  $a_1 = 0.5$ .

### C. Relay element in a first-order system.

The system was of the form given by (20) with  $f_0(x)$  denoting the relay element and  $a_1 = 1.0$ . The simulation of the relay was accomplished by simulating the coulomb friction type nonlinearity and then inverting the output of it. The simulation diagram for the coulomb friction is shown in Fig. B-3. The simulated nonlinear function is shown in Fig. 3-16. Fig. 3-17 shows the calculated nonlinear function corresponding to minimum area of the plot at an input frequency of 0.1 rad/sec. The area enclosed by the plot was minimum when the linear coefficient was equal to one.

The identification of this nonlinearity is not as close as the identification of the two previous nonlinearities. This is due to the nature of the nonlinearity. The large discontinuity in slope causes the generation of more harmonics. The filter eliminates or attenuates the harmonics that are outside the passband of the filter. Thus the elimination or attenuation of more harmonics in the case of relay type nonlinearity than in the other two cases produces a less accurate calculation of the nonlinear function.

In all these cases of single-valued nonlinearities, Kohr's criterion of minimum area of the plot identified the nonlinear function as well as the linear coefficient and was demonstrated to be correct.



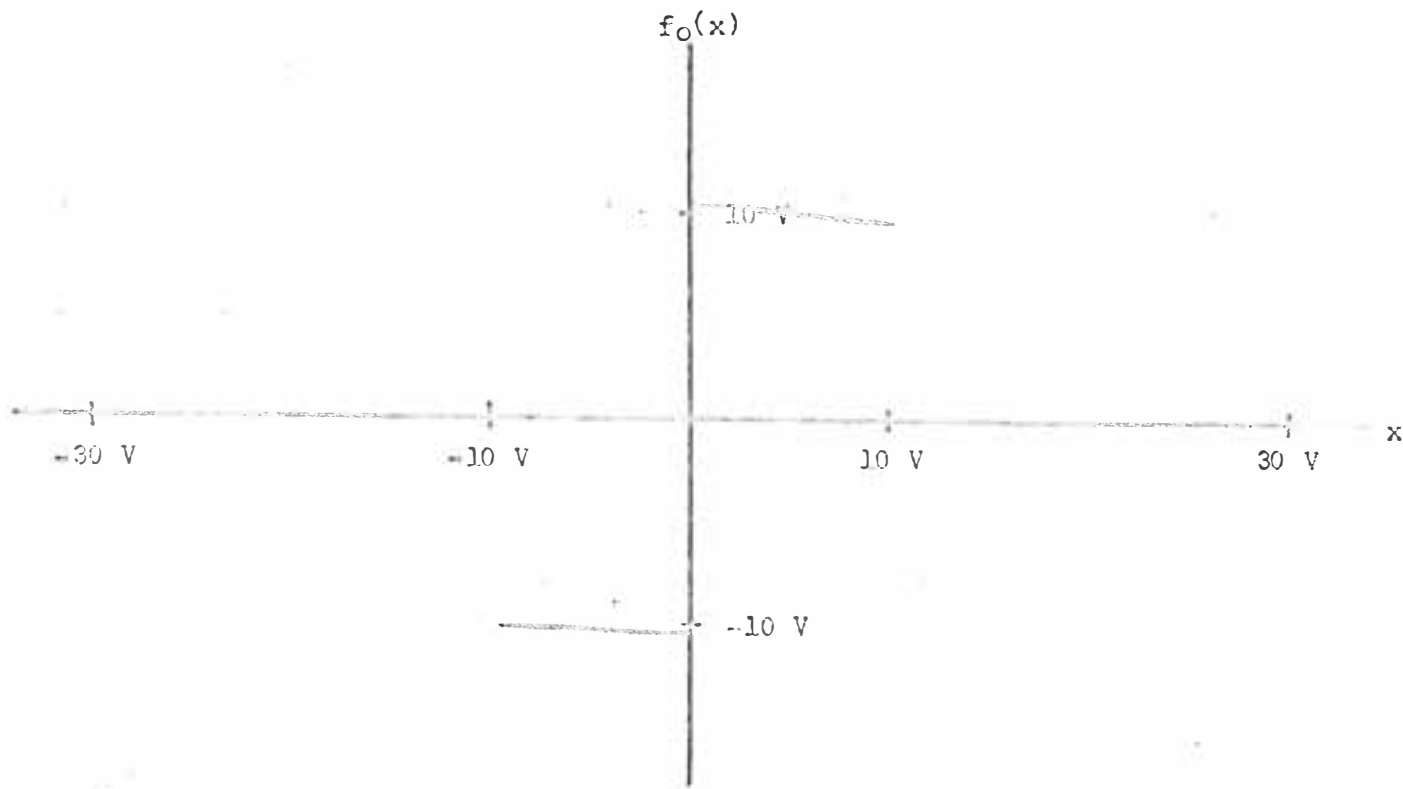


Fig. 3-16. Simulated relay type nonlinearity.

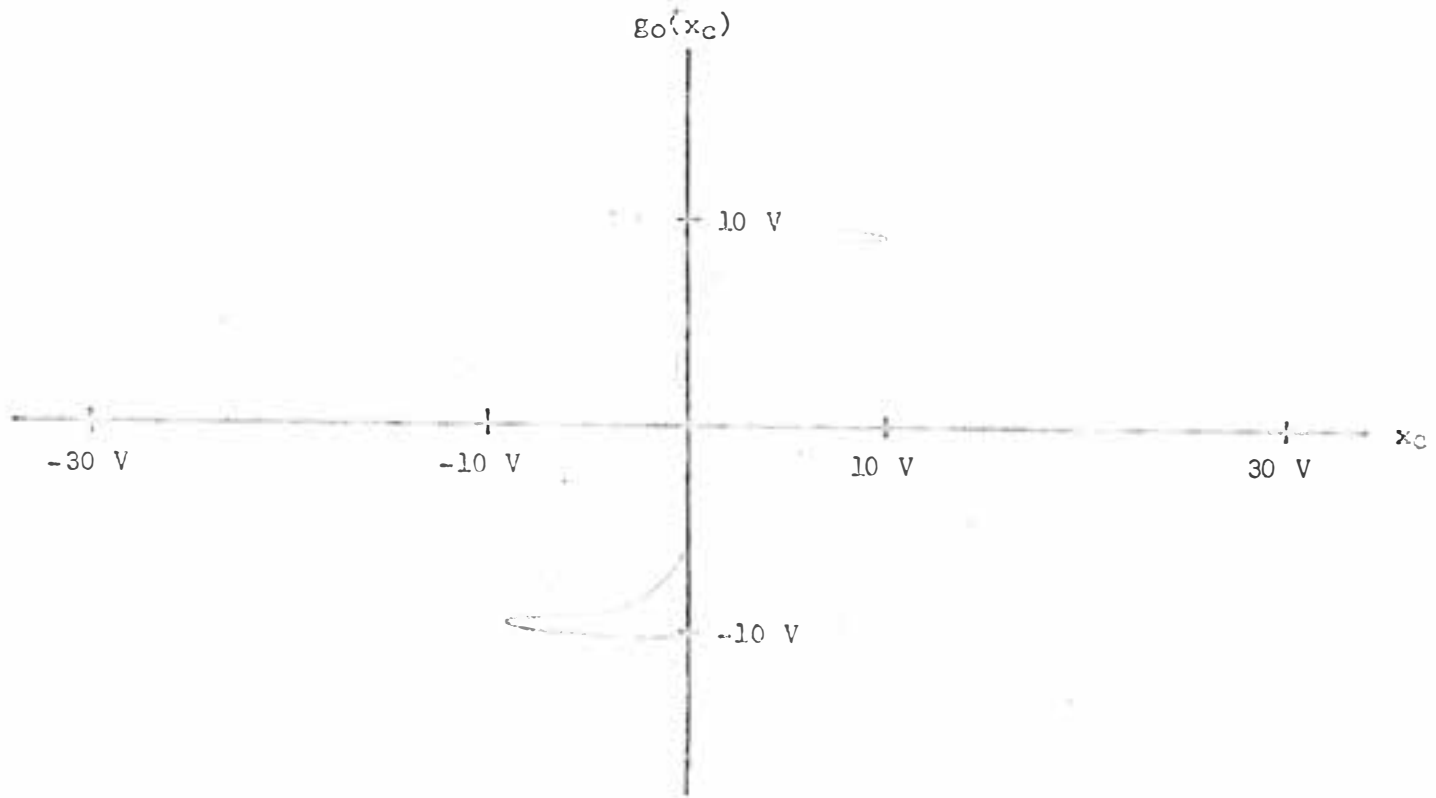


Fig. 3-17. Calculated nonlinear function (relay) for  $\omega = 0.1$  rad/sec and  $a_1 = 1.0$ .

CHAPTER IV  
KOHR'S METHOD APPLIED TO SYSTEMS CONTAINING  
DOUBLE-VALUED NONLINEARITIES

Kohr<sup>3</sup> states that the criterion of minimum area of the plot identifies systems having double-valued nonlinearities as well. Hence Kohr's method was applied to a first-order system containing a memory-type nonlinearity. The resulting plots, obtained by use of Kohr's method, are shown in Figures 4-1 through 4-6, and discussed in this chapter.

The system to be identified was of the form  $a_1 p x + f_0(x) = y$ , where  $a_1 = 1.0$ ,  $f_0(x)$  represents the backlash-type nonlinear element, and  $y$  is the sinusoidal input. Second-order filters were used in the identification with the corresponding ITAE coefficients. The cutoff frequency used in the filters was 1.0 rad/sec. The frequency of the sinusoidal input applied to the system was 0.1 rad/sec.

To start with, the linear coefficient  $a_1$ , to be determined, was set up arbitrarily as 1.5. The corresponding plot of the nonlinear function is shown in Fig. 4-3. Then the coefficient  $a_1$  was increased to 2.0. Fig. 4-2 represents the calculated nonlinear function when  $a_1 = 2.0$ . From Figures 4-2 and 4-3, it is obvious that the area enclosed by the plot increases when the coefficient  $a_1$  is increased from 1.5 to 2.0. According to Kohr, the minimum area of the plot identifies the nonlinear function and determines the linear coefficient or coefficients, as the case may be. In this case, only one linear coefficient,  $a_1$ , is to be determined. So the linear coefficient  $a_1$  was

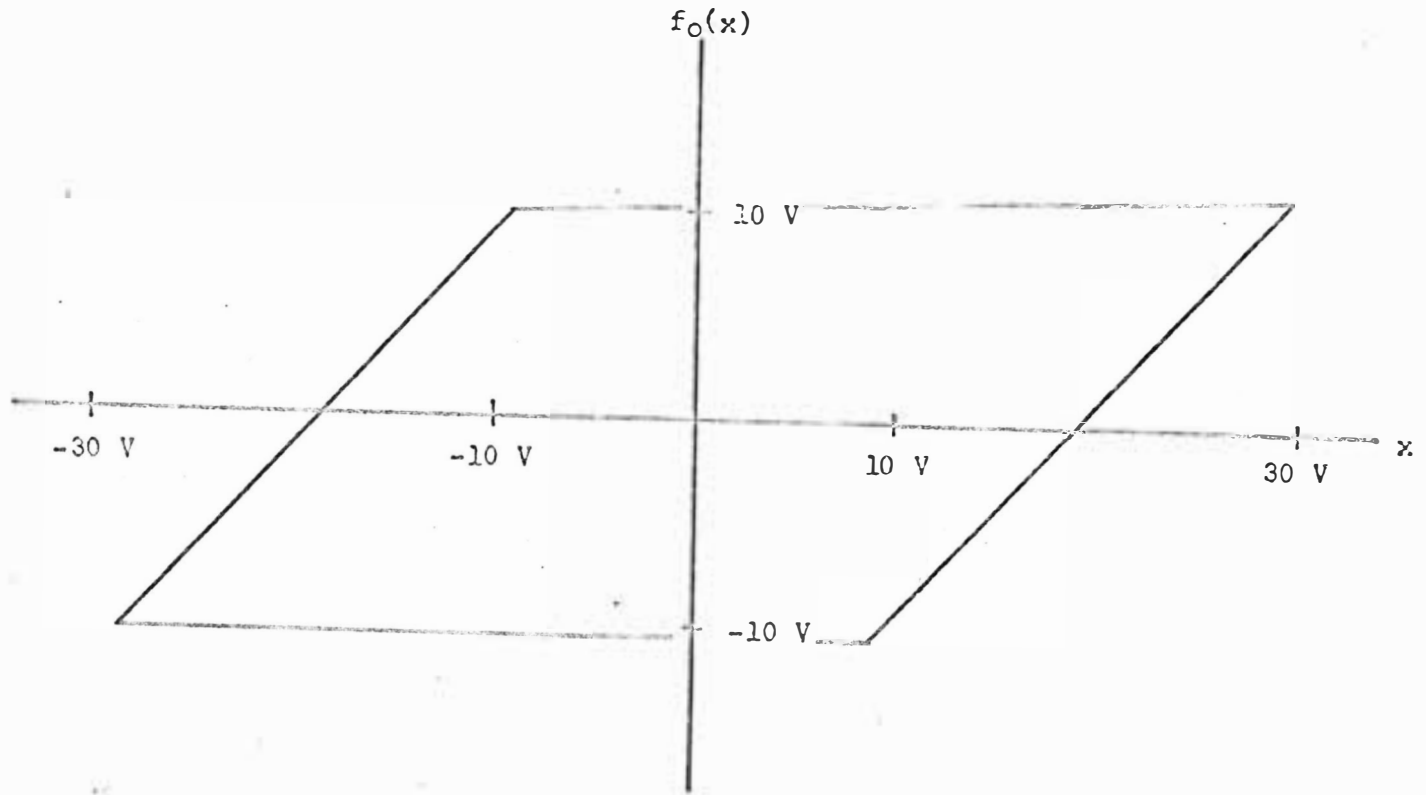


Fig. 4-1. Simulated backlash type nonlinearity.

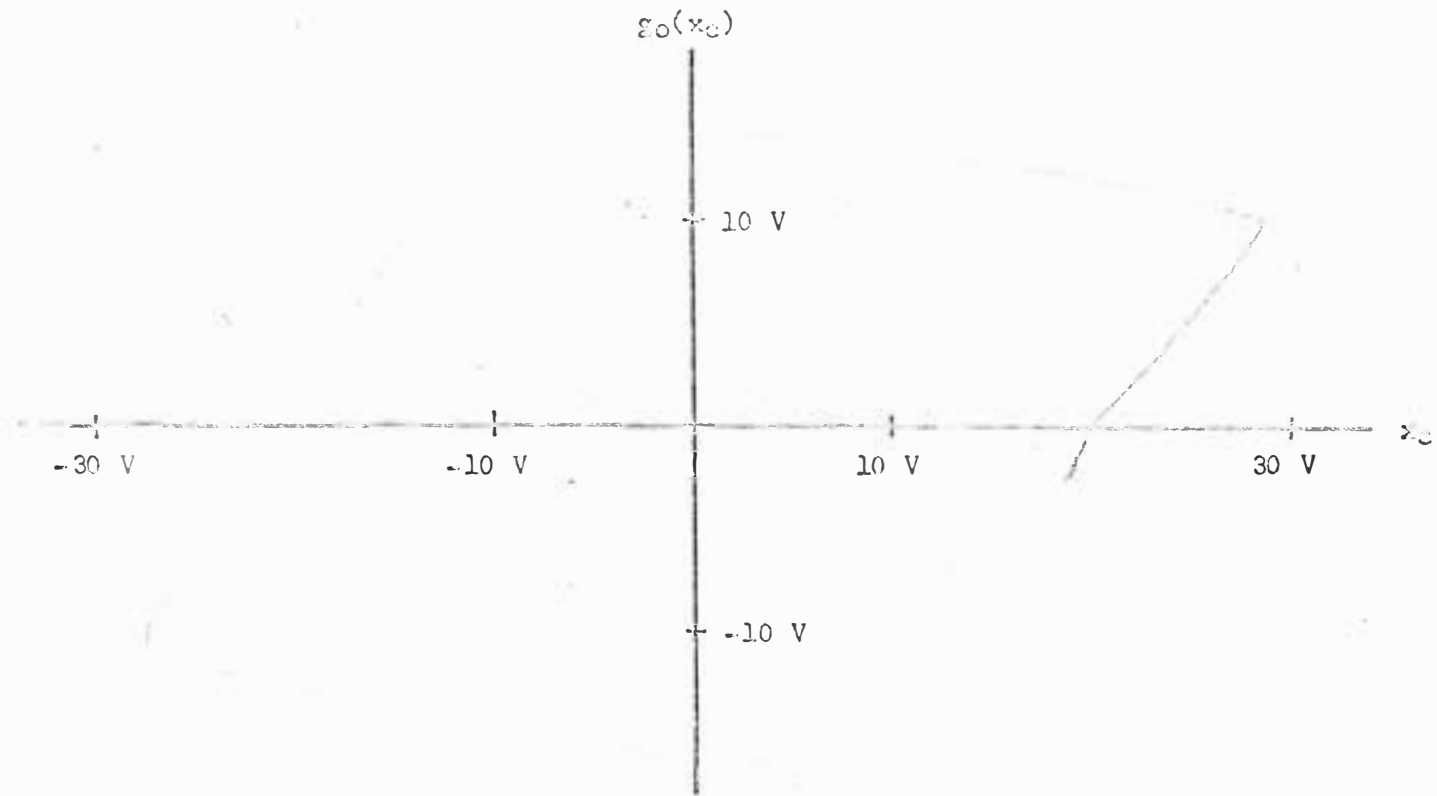


Fig. 4-2. Calculated nonlinear function (backlash) for  $\omega = 0.1$  rad/sec, and  $a_1 = 2.0$ .

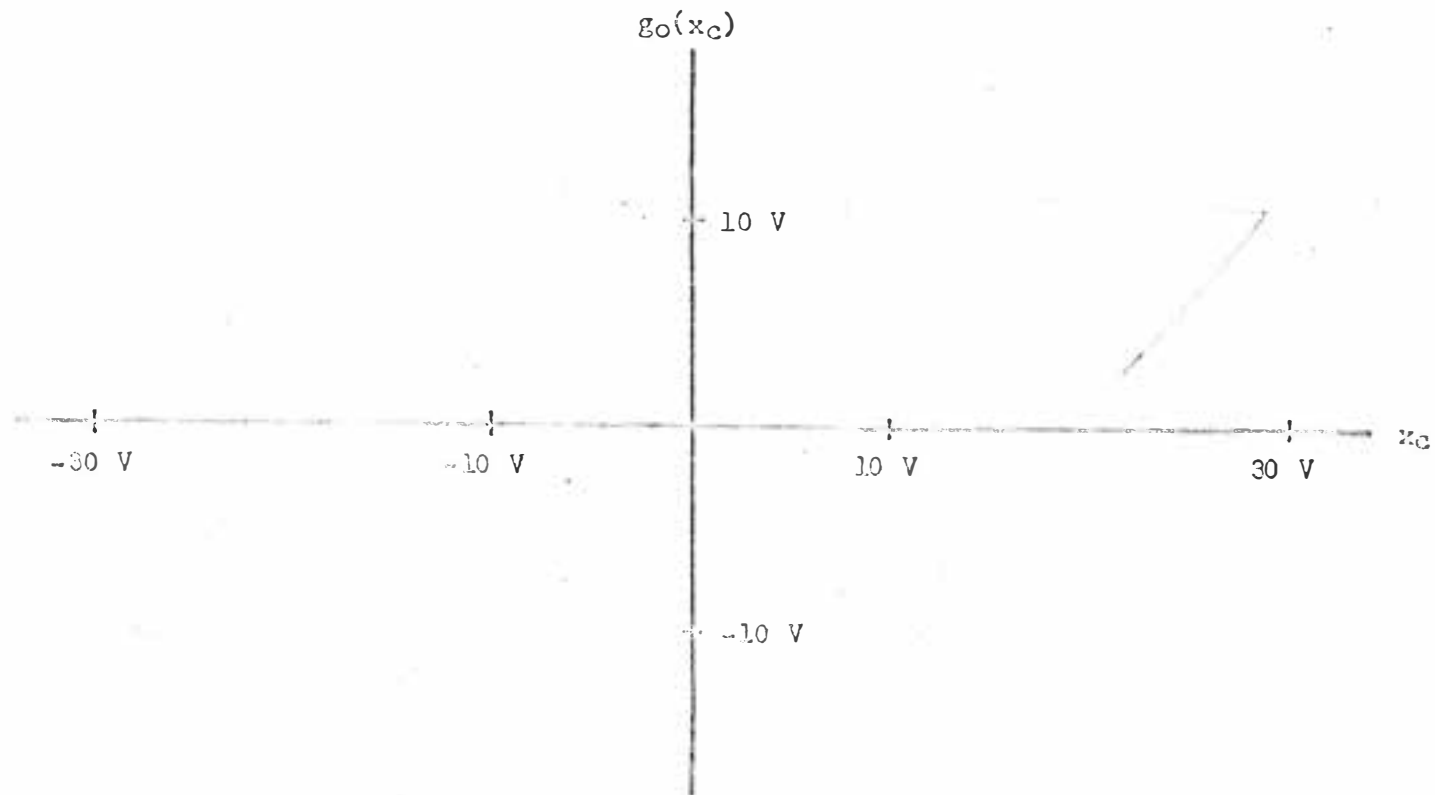


Fig. 4-3. Calculated nonlinear function (backlash) for  $\omega = 0.1$  rad/sec, and  $a_1 = 1.5$ .

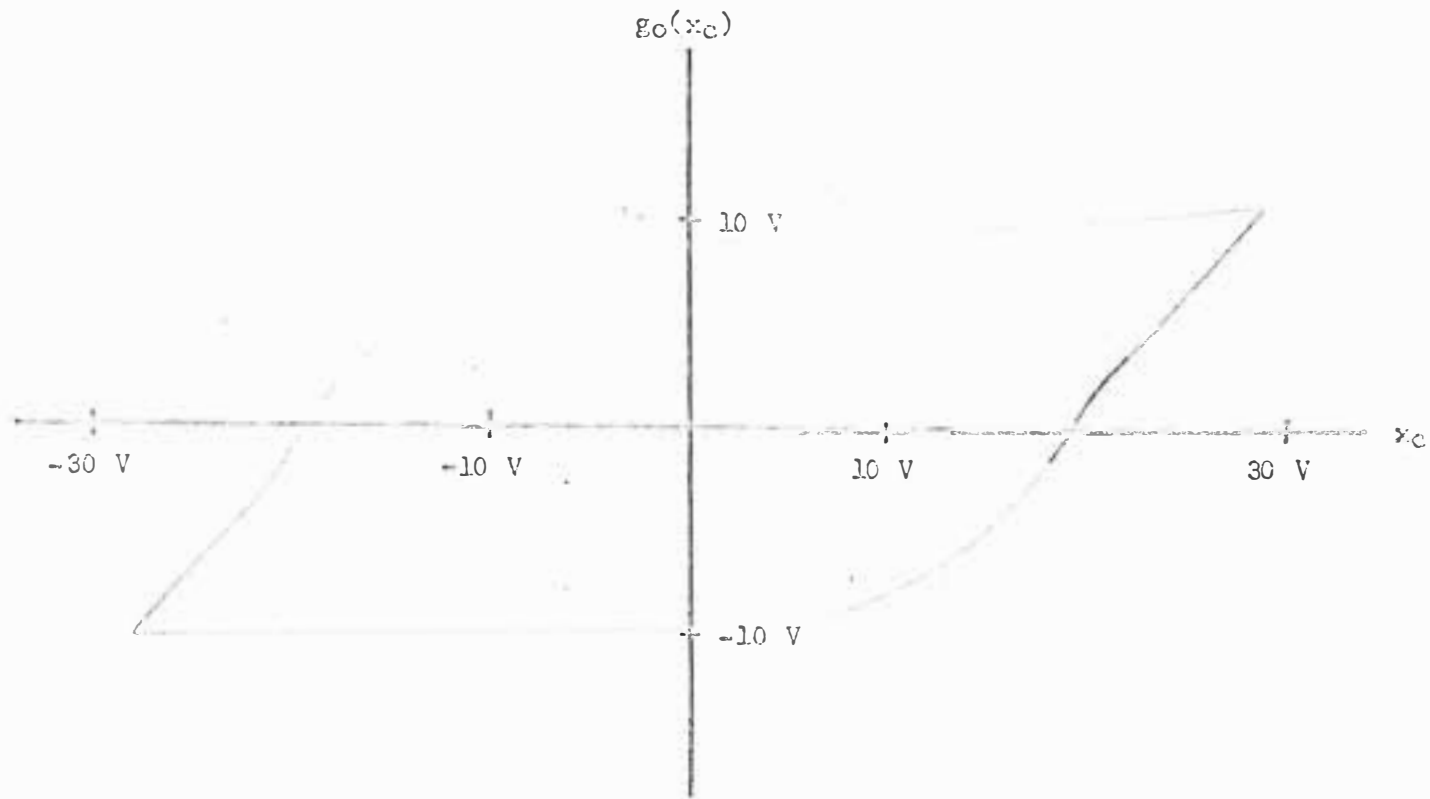


Fig. 4-4. Calculated nonlinear function (backlash) for  $\omega = 0.1\text{ rad/sec}$ , and  $a_1 = 1.0$ .

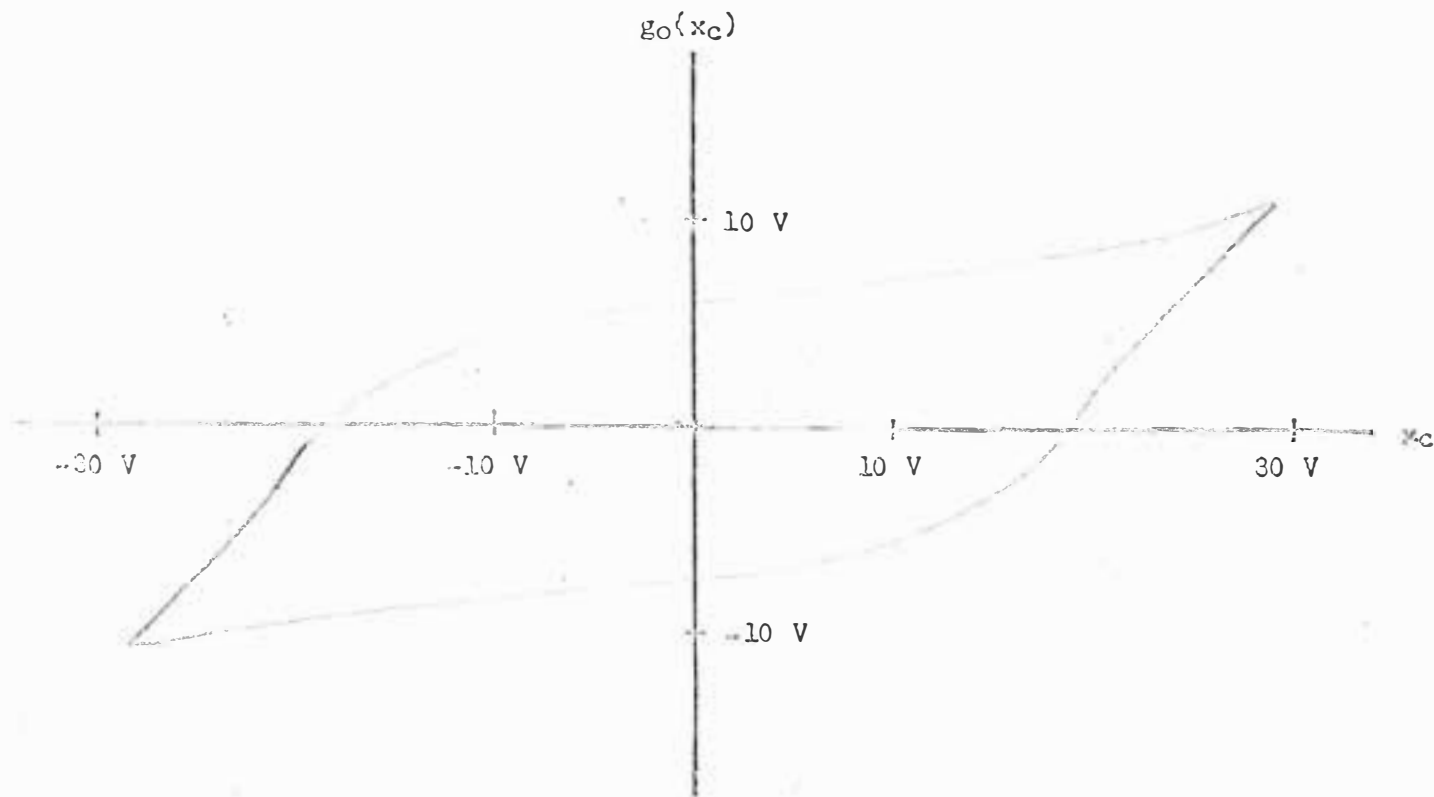


Fig. 4-5. Calculated nonlinear function (backlash) for  $\omega = 0.1$  rad/sec, and  $a_1 = 0.5$ .



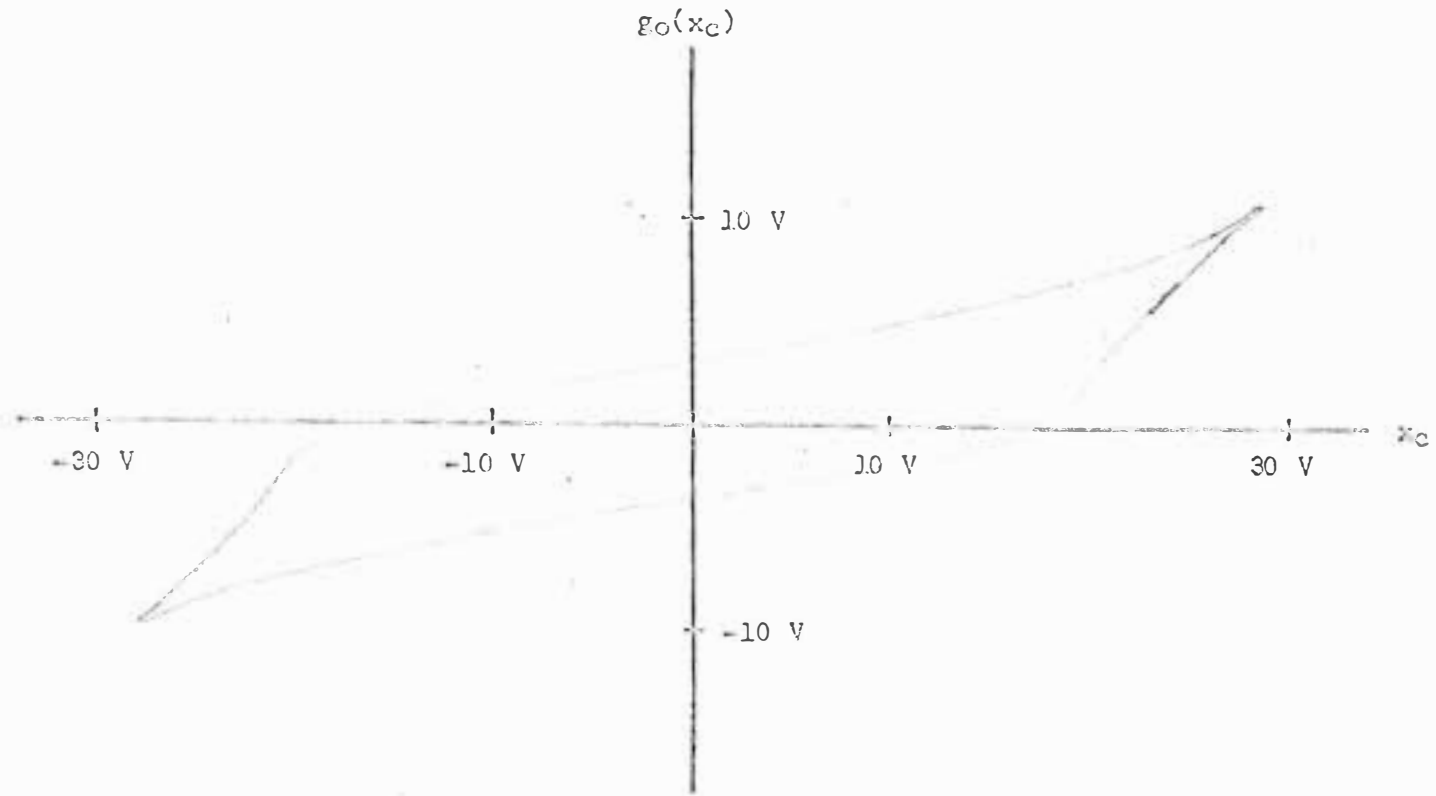


Fig. 4-6. Calculated nonlinear function (backlash) for  $\omega = 0.1$  rad/sec, and  $a_1 = 0.0$ .

reduced gradually and the corresponding plots were taken. The area enclosed by the plot went on decreasing as the linear coefficient was decreased. The  $g_0(x_c)$  vs  $x_c$  plots corresponding to  $a_1 = 1.0$ ,  $0.5$ , and  $0.0$  are shown in Figures 4-4, 4-5, and 4-6, respectively. The area enclosed by the plot was minimum when  $a_1 = 0.0$  and it can be verified from the figures shown. Hence, according to Kohr's criterion, the calculated linear coefficient is zero, and the corresponding  $g_0(x_c)$  vs  $x_c$  plot represents the calculated nonlinear function.

By comparing with the actual nonlinear function shown in Fig. 4-1, it may be observed that the plot corresponding to  $a_1 = 1.0$ , approximates more closely the nonlinear function than the plot corresponding to  $a_1 = 0.0$ . Also, the actual linear coefficient is equal to one and not zero. Thus the criterion of minimum area of the plot, as suggested by Kohr, neither identifies the nonlinear function nor determines the linear coefficient. However, it does reveal the nature of the double-valued nonlinearity in the system.

Thus it is shown that the criterion of minimum area of the plot does not apply to systems which contain a memory-type, or double-valued nonlinearity while the criterion is substantiated for systems containing single-valued nonlinearities.

## CHAPTER V

## DETERMINATION OF THE ORDER OF THE SYSTEM

Kohr<sup>3</sup> mentions that the inability to determine the order of the system to be identified is a major limitation in his method. If the location of the nonlinearity is known, then the order of the system may be determined by a procedure suggested in this chapter. The procedure is an extension of the technique used by Kohr in identifying nonlinear systems. If the procedure is to be successful, the nonlinearity in the system must be single-valued since Kohr's method, as has been shown, identifies only the systems with single-valued nonlinearities.

If the system is of the form of equation (1) and the assumed differential equation is of the form of equation (15), then the error equation established would be of the form of equation (16), which is reproduced below.

$$g_k(p^k x_c) - L(p)f_k(p^k x) = (a_n - b_n)p^n x_c + \dots + (a_{k+1} - b_{k+1})p^{k+1} x_c + (a_{k-1} - b_{k-1})p^{k-1} + \dots + (a_1 - b_1)p x_c + (a_0 - b_0)x_c$$

If the coefficient of the zeroth derivative of the output is the nonlinear coefficient then the error equation becomes

$$g_0(x_c) - L(p)f_0(x) = (a_n - b_n)p^n x_c + (a_{n-1} - b_{n-1})p^{n-1} x_c + \dots + (a_k - b_k)p^k x_c + \dots + (a_3 - b_3)p^3 x_c + (a_2 - b_2)p^2 x_c + (a_1 - b_1)p x_c \quad (16a)$$

If the system to be identified is of third order, then the coefficients of the derivatives higher than third are zero; i.e., the coefficients  $a_4, a_5, \dots, a_n$  are zero. The area of the  $g_0(x_c)$  vs  $x_c$  plot would be

minimum when

$$a_1 = b_1$$

$$a_2 = b_2$$

$$\vdots$$

$$a_{n-1} = b_{n-1}$$

$$a_n = b_n$$

Since  $a_4, a_5, \dots, a_n$  are all equal to zero, the area of the  $g_0(x_c)$  vs  $x_c$  plot would be minimum when  $b_4, b_5, \dots, b_n$  are all equal to zero, and

$$a_1 = b_1$$

$$a_2 = b_2$$

$$a_3 = b_3$$

Thus if the calculated coefficients  $b_{k+1}, b_{k+2}, \dots, b_n$  are all equal to zero, then the system is determined to be of  $k^{\text{th}}$  order.

The procedure is explained with an example, and is illustrated with experimental results. Let the system, whose order is to be determined, be a first-order system of the form  $a_1 p x + f_0(x) = y$ , where  $a_1 = 1.0$ ,  $f_0(x)$  is the single-valued nonlinear function,  $y$  is the sinusoidal input, and  $x$  is the output. If the approximate order of the system is known, then it helps to simplify the procedure. The system mentioned above is assumed to be of second order, and third-order linear filters with ITAE coefficients were used in the identification scheme. Thus the derivatives of the filtered output up to third order were available from the filter. The cutoff frequency of the linear filters used was 1.0 rad/sec. The difference between the simulation scheme

shown in Fig. A-1 and the simulation scheme used in this example is the order of the filters and the subsequent changes. Let  $b_1$ ,  $b_2$ , and  $b_3$  be the coefficients of the first-, second-, and third-order derivatives of the filtered output  $x_c$  respectively. The coefficients  $b_1$ ,  $b_2$ , and  $b_3$  were controlled by potentiometers individually.

The coefficients  $b_1$ ,  $b_2$ , and  $b_3$  were adjusted by varying the potentiometers to give a minimum area of the plot  $g_o(x_c)$  vs  $x_c$ , according to the procedure given in Chapter II to determine linear coefficients for higher order systems.

Initially, all the three coefficients were set arbitrarily at 2.0. The calculated nonlinear function was plotted for those values (Fig. 5-1). Then the coefficient of the first derivative,  $b_1$ , was adjusted for minimum area of the plot. Fig. 5-2 ( $b_1 = 1.0$ ,  $b_2 = 2.0$ , and  $b_3 = 2.0$ ) represents the corresponding plot. The coefficient of the second derivative,  $b_2$ , was next adjusted keeping  $b_1 = 1.0$ , and  $b_3 = 2.0$ . The area was minimum when  $b_2$  was zero and the plot is shown in Fig. 5-3. Finally the coefficient of the third derivative,  $b_3$ , was varied for minimum area of the plot keeping  $b_1$  and  $b_2$  at 1.0 and 0, respectively. The area was minimum when  $b_3$  was zero. Fig. 5-4 shows the plot. The procedure was repeated till the coefficients attained unchanging values. On the very second iteration this result was achieved. The final plot was the same as Fig. 5-4, corresponding to  $b_1 = 1.0$ ,  $b_2 = 0.0$ , and  $b_3 = 0.0$ .

When the calculated values of the linear coefficients are known, the order of the system may be determined. In this system, for

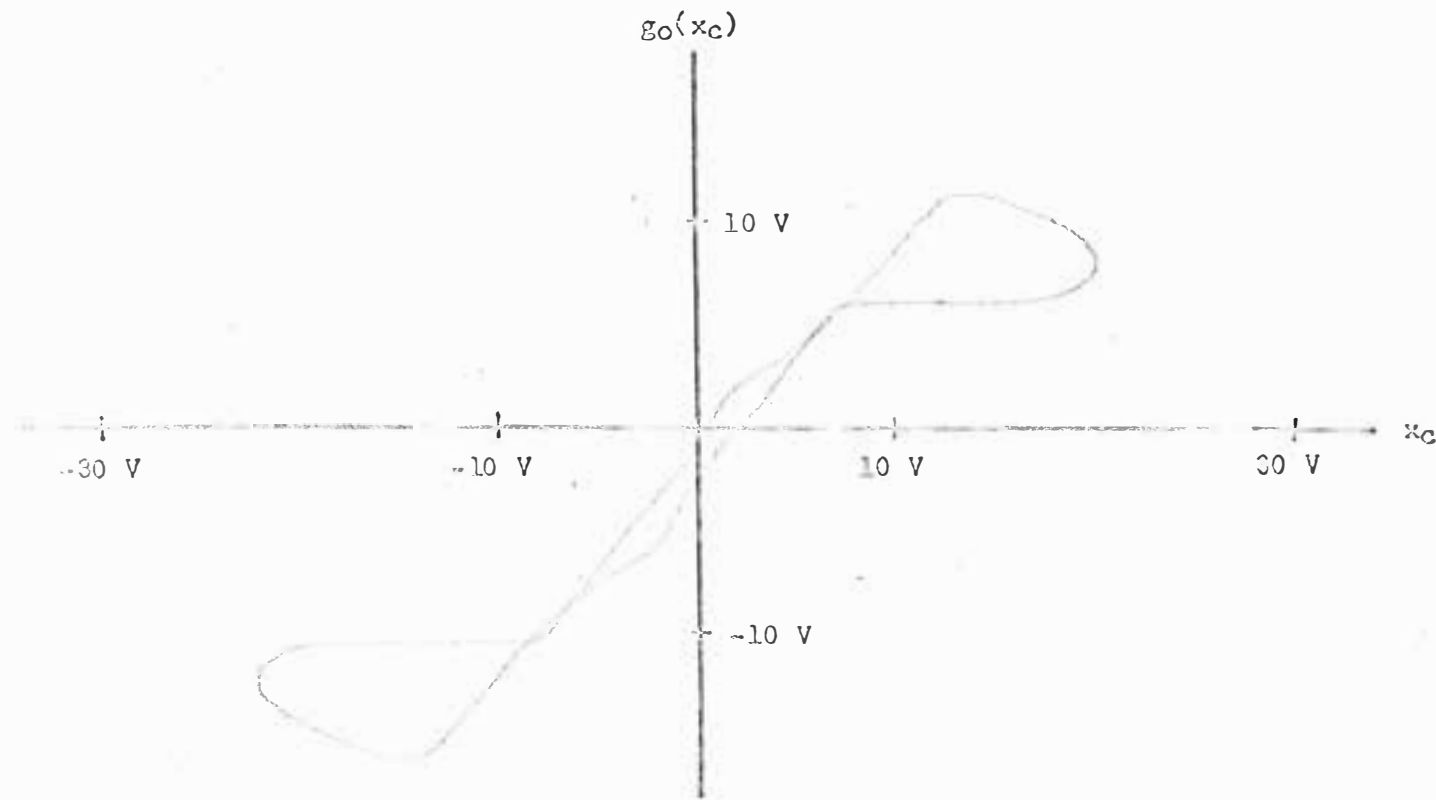


Fig. 5-1. Calculated nonlinear function for  $b_1 = 2.0$ ,  $b_2 = 2.0$ , and  $b_3 = 2.0$ .

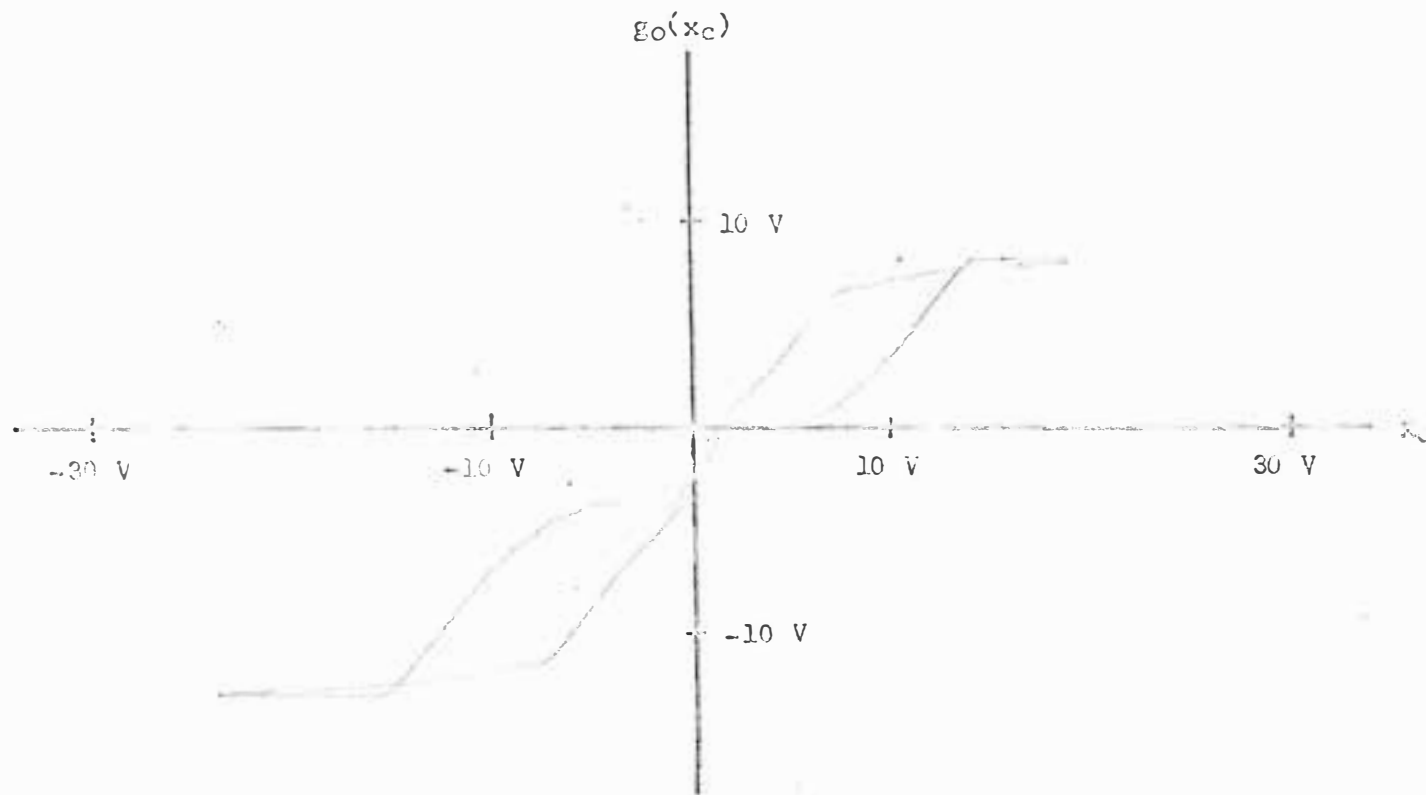


Fig. 5-2. Calculated nonlinear function for  $b_1 = 1.0$ ,  $b_2 = 2.0$ , and  $b_3 = 2.0$ .

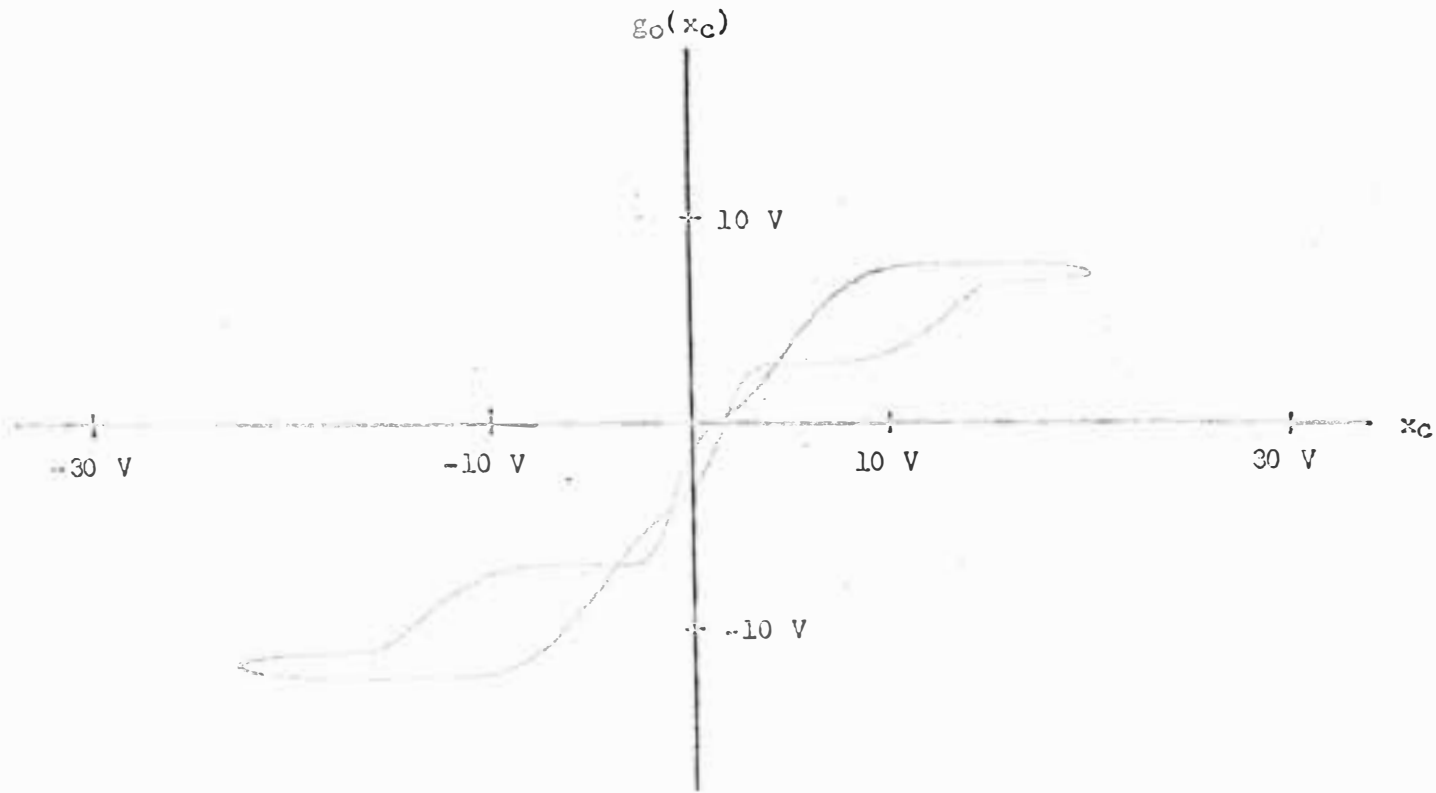


Fig. 5-3. Calculated nonlinear function for  $b_1 = 1.0$ ,  $b_2 = 0.0$ , and  $b_3 = 2.0$ .



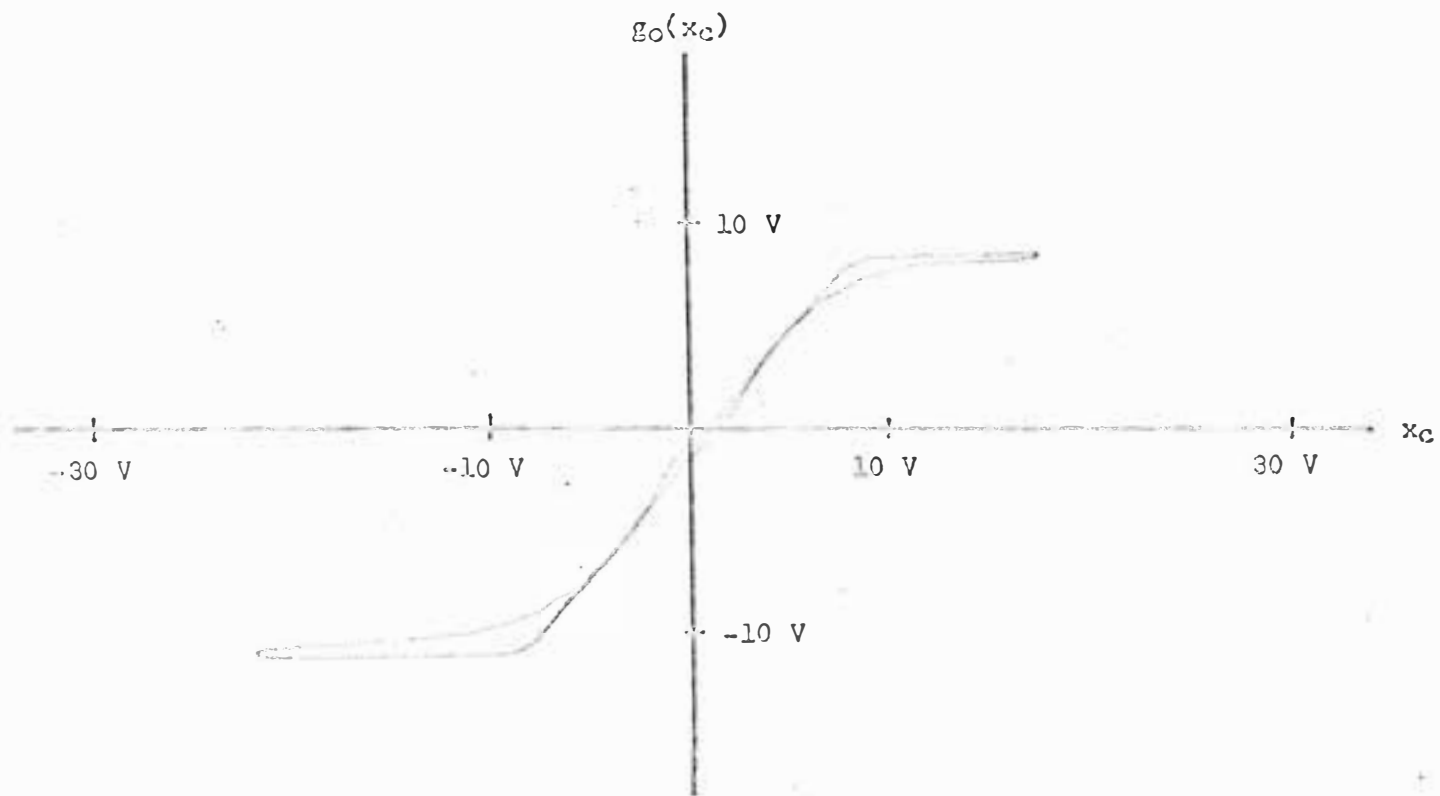


Fig. 5-4. Calculated nonlinear function for  $b_1 = 1.0$ ,  $b_2 = 0.0$ , and  $b_3 = 0.0$ .

example, the calculated coefficients of the second- and third-order derivatives of the filtered output are zero, indicating thereby the system to be of first order. Thus the order of the system has been correctly determined by this procedure. As a further check, a plot (Fig. 5-5) was taken for  $b_1 = 1.0$ ,  $b_2 = 1.0$ , and  $b_3 = 1.0$ , an arbitrary set of intermediate values. Fig. 5-6 shows the plot corresponding to  $b_1 = 0.0$ ,  $b_2 = 0.0$ , and  $b_3 = 0.0$ . It is evident from the figures that the area enclosed in both these plots is individually greater than the area enclosed by the plot shown in Fig. 5-4.

If the estimated or assumed order is lower than the actual order of the system, then the coefficient of the highest order derivative of the filtered output will not be zero for minimum enclosed area in the plot. A higher order filter should then be used and the procedure repeated till the coefficient of the highest order derivative of the filtered output is obtained as zero corresponding to minimum area of the plot.

The identification technique may sometimes give erroneous results, if the order of the system is not determined. For example, if a fifth-order system to be identified is assumed to be of third order, then the calculated linear coefficients will be in error since the coefficients of the fourth and fifth derivatives are completely ignored in the calculation.

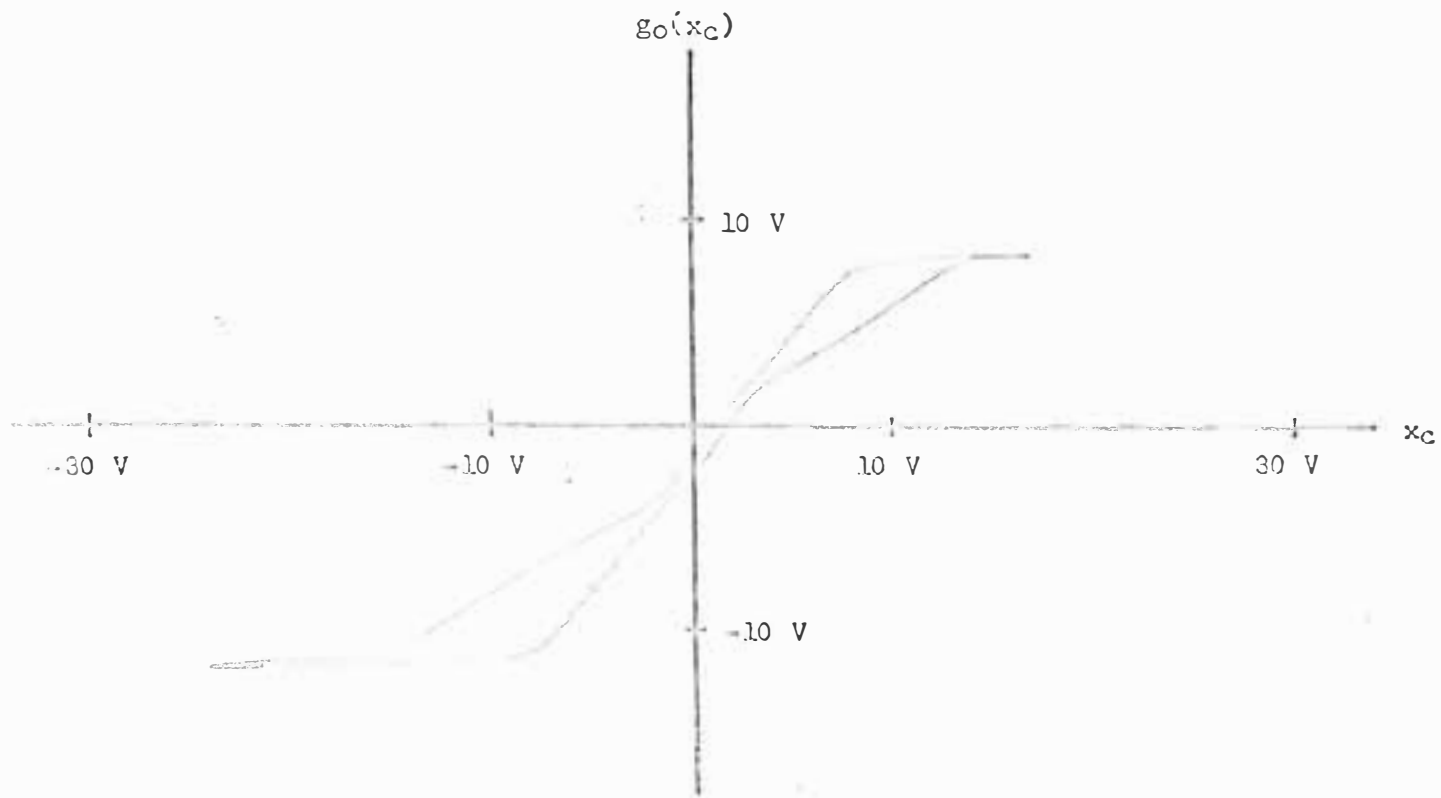


Fig. 5-5. Calculated nonlinear function for  $b_1 = 1.0$ ,  $b_2 = 1.0$ , and  $b_3 = 1.0$ .

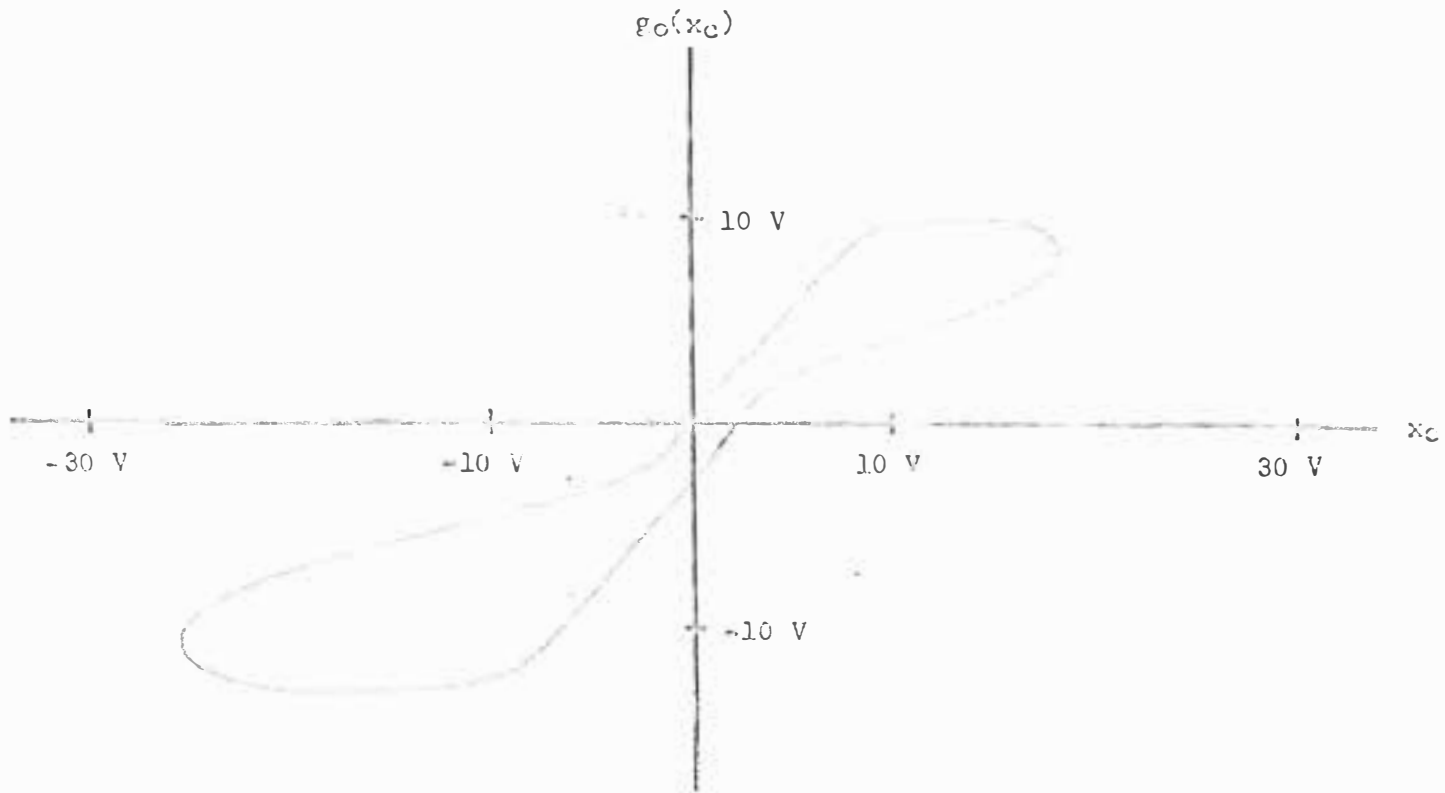


Fig. 5-6. Calculated nonlinear function for  $b_1 = 0.0$ ,  $b_2 = 0.0$ , and  $b_3 = 0.0$ .

## CHAPTER VI

## CONCLUSIONS

It has been verified that Kohr's criterion of minimum area of the plot gives satisfactory results in the identification of nonlinear systems containing single-valued nonlinearities, and that it does not apply to systems containing double-valued nonlinearities. Consequently, the procedure given by Kohr for identifying a system which contain more than one nonlinearity will give erroneous results, if one of the nonlinearities is double-valued.

According to Kohr, determining the order of the system to be identified and the location of the nonlinearity within the system are the two major limitations of his method. In case no previous information about the location of the nonlinearity is available, the location of the nonlinearity must be assumed. If the location of the nonlinearity is correctly assumed, then the calculation would result in a satisfactory identification. Otherwise a satisfactory solution may not result.

A procedure has been suggested in Chapter V for determining the order of the system, when the location of the nonlinearity is known. The procedure may be tested for higher order systems where some of the linear coefficients of the intermediate derivatives are zero, and is suggested for further work.

It is desirable to have a cutoff frequency of 1.0 rad/sec for the linear filter since the low cutoff frequency would help to reduce errors due to noise above the cutoff frequency. Of course, very low-frequency noise which lies in the passband of the filter cannot be reduced. Also,

a cutoff frequency of 1.0 rad/sec simplifies the scaling procedure for the filter. Assuming that the loop gain is equally distributed among the integrators, their outputs will be  $p^k x_c / \omega_0^k$ . When  $\omega_0$  is equal to 1.0, the outputs of the integrators will become  $p^k x_c$ . Thus a cutoff frequency of 1.0 rad/sec makes the derivatives available directly as the outputs of integrators, thereby eliminating the use of additional amplifiers.

The calculated nonlinear function may not be accurate due to the use of finite approximation of the transport lag and because of noise in the system. The quality of the transport lag approximation deteriorates with increasing frequency. When the input frequency is increased, the frequencies of the harmonics are also increased correspondingly. Thus an increase in the input frequency causes more harmonics of the output to be filtered out. Hence, a satisfactory identification will not result if the input frequency exceeds a certain limit. This limit depends upon the nature of the nonlinearity since the harmonics in the output are generated by the nonlinearity in the system. A relay type nonlinearity generates more harmonics than a saturating type nonlinearity.

An input frequency of one-tenth of the cutoff frequency of the filter usually results in satisfactory calculation of the nonlinear function. Random inputs as well as periodic inputs which satisfy this requirement may be used in the identification of nonlinear systems. Periodic inputs may be preferred since they can be depended upon to reach a certain magnitude within a specified time. This is especially

true in the case where a large amplitude is required for the nonlinear function to be completely revealed. In this case, random inputs may require a longer time to complete the calculation, since the magnitude varies randomly with respect to time.

The amplitude of the input signal should be of sufficient magnitude to reveal the complete nonlinear function. But it is difficult to estimate the required magnitude. Hence, to start with, the maximum possible input signal should be applied without overloading any of the amplifiers.

The results may be obtained using Butterworth coefficients (Table 2) and compared with the results obtained using ITAE coefficients in the filters. Another approximation may also be used for the transport lag by expressing  $e^{-Ts}$  as

$$\frac{e^{-Ts/2}}{e^{+Ts/2}}$$

and truncating the corresponding the infinite series in the numerator as well as in the denominator.  $T$  depends on the cutoff frequency chosen. For want of sufficient number of analog computer amplifiers, the implementation of the above-mentioned transport lag approximation was not possible.

It may be noted, from the tables given in Appendix C, that for first- and second-order filters, Butterworth and ITAE coefficients are the same. The coefficients begin to differ for filters higher than the second order.

In this work, it is shown that the claim made by Kohr pertaining to the successful identification of systems containing either single-

valued or double-valued nonlinearities is only partially correct. The criterion given by Kohn has been verified to be true for the identification of systems containing single-valued nonlinearities only. Though Kohn states that the method has been used successfully to determine memory-type nonlinear functions, he has not presented the experimental results to support his assertion. In this thesis experimental results are presented which indicate that Kohn's criterion reveals only the nature of the double-valued nonlinearity. It is also shown that the criterion does not determine the linear coefficients or the double-valued nonlinear function exactly. A procedure has been suggested in this work for determining the order of the system which might obviate one of the major limitations of Kohn's method.



## REFERENCES

1. M. Shinbrot, "On the Analysis of Linear and Nonlinear Systems," Trans. ASME, Vol. 79, April 1957, pp. 547-552.
2. A. B. Clymer, "Direct System Synthesis by Means of A Computer," Trans. AIEE, Vol. 77, Part 1, January 1959, pp. 798-806.
3. R. H. Kohn, "A Method for the Determination of a Differential Equation Model for Simple Nonlinear Systems," IEEE Trans. on Electronic Computers, Vol. EC-12, No. 4, 1963, pp. 394-400.
4. C. Giese and R. B. McGhee, "Estimation of Nonlinear System States and Parameters by Regression Methods," Joint Automatic Control Conference Preprints, 1965, pp. 46-53.
5. D. M. Detchmendy and R. Sridhar, "Sequential Estimation of States and Parameters in Noisy Nonlinear Dynamical Systems," Joint Automatic Control Conference Preprints, 1965, pp. 56-63.
6. K. K. Graupe, "The Analog Solution of Some Functional Analysis Problems," Trans. AIEE, Vol. 79, Part 1, 1960, pp. 793-799.
7. K. S. Narendra and P. G. Gallman, "An Iterative Method for the Identification of Nonlinear Systems Using a Hammerstein Model," IEEE Trans. on Automatic Control, July 1966, pp. 546-550.
8. M. V. Mathews and W. W. Seifert, "Transfer Function Synthesis with Computer Amplifiers and Passive Networks," Proc. Western Joint Computer Conference, 1955, pp. 7-12.
9. D. Graham and R. C. Lathrop, "The Synthesis of 'Optimum' Transient Response: Criteria and Standard Forms," Trans. AIEE, Vol. 72, Part II, November 1953, pp. 273-283.
10. L. I. Hoberock and R. H. Kohn, "An Experimental Determination of Differential Equations to Describe Simple Nonlinear Systems," Joint Automatic Control Conference Preprints, 1966, pp. 616-623.
11. L. A. Zadeh, "On the Identification Problem," IRE Trans. on Circuit Theory, December 1955, pp. 277-281.
12. "Berkeley Electronic Analog Simulating Equipment Instruction Manual," Beckman Instruments, Inc., 1954, pp. 3.21-3.29.
13. C. L. Johnson, Analog Computer Techniques, McGraw-Hill Book Company, Inc., 1956, pp. 45-63 and 107-132.

14. B. C. Kuo, Automatic Control Systems, Prentice-Hall, Inc., 1962, pp. 467-469.
15. G. R. Peterson, Basic Analog Computation, The Macmillan Company, 1967.
16. Dunstan Graham and Duane McRuer, Analysis of Nonlinear Control Systems, John Wiley and Sons, Inc., 1961.
17. John E. Gibson, Nonlinear Automatic Control, McGraw-Hill Book Company, 1968.
18. C. A. Stewart and R. Atkinson, Basic Analogue Computer Techniques, McGraw-Hill Publishing Company Limited, 1967, pp. 75-95.
19. Robert C. Weyrick, Fundamentals of Analog Computers, Prentice-Hall, Inc., 1969, pp. 133-135.
20. J. N. Warfield, Introduction to Electronic Computers, Prentice-Hall, Inc., 1959, pp. 82-84.

## APPENDICES

APPENDIX A  
 SIMULATION SCHEME FOR THE IDENTIFICATION  
 OF FIRST-ORDER NONLINEAR SYSTEM

A general simulation diagram for the identification of first-order system,  $a_1 \dot{x} + f_0(x) = y$ , is shown in Fig. A-1; where  $a_1 = 1$ , is the linear coefficient,  $f_0(x)$  is the nonlinear coefficient and  $y$  is the sinusoidal input to the system.

The system,  $\dot{x} = y - f_0(x)$  is simulated using amplifiers 4 and 5 as well as the simulated nonlinear coefficient. The input to integrator 4 is  $\dot{x}$  i.e.,  $y - f_0(x)$ , and its output is  $-x$ , which is inverted by amplifier 5 to get the system output,  $x$ . Output of integrator 2 is the sinusoidal input,  $y$ , to the system. The filtered output,  $x_c$ , and its derivative are obtained using a second-order linear filter comprising amplifiers 6, 7, 8, and 9. Output of integrator 8 gives the filtered output,  $x_c$ , and integrator 7 gives the first derivative,  $\dot{x}_c$ , of the filtered output. The input,  $y$ , also is passed through a similar filter, comprising amplifiers 11, 12, 13, and 14; the output of amplifier 13 gives the filtered input,  $-y_c$ .

From the simulation diagram, it is evident that the output of amplifier 15 is  $y_c - a_1 \dot{x}_c$  i.e.,  $g_0(x_c)$ . Thus the  $g_0(x_c)$  vs  $x_c$  plot may be obtained using this simulation scheme and the system may be identified. ITAE second-order coefficients and a cutoff frequency of one radian per second are used in the linear filters. The simulation diagrams of five different nonlinearities are given in Appendix B.

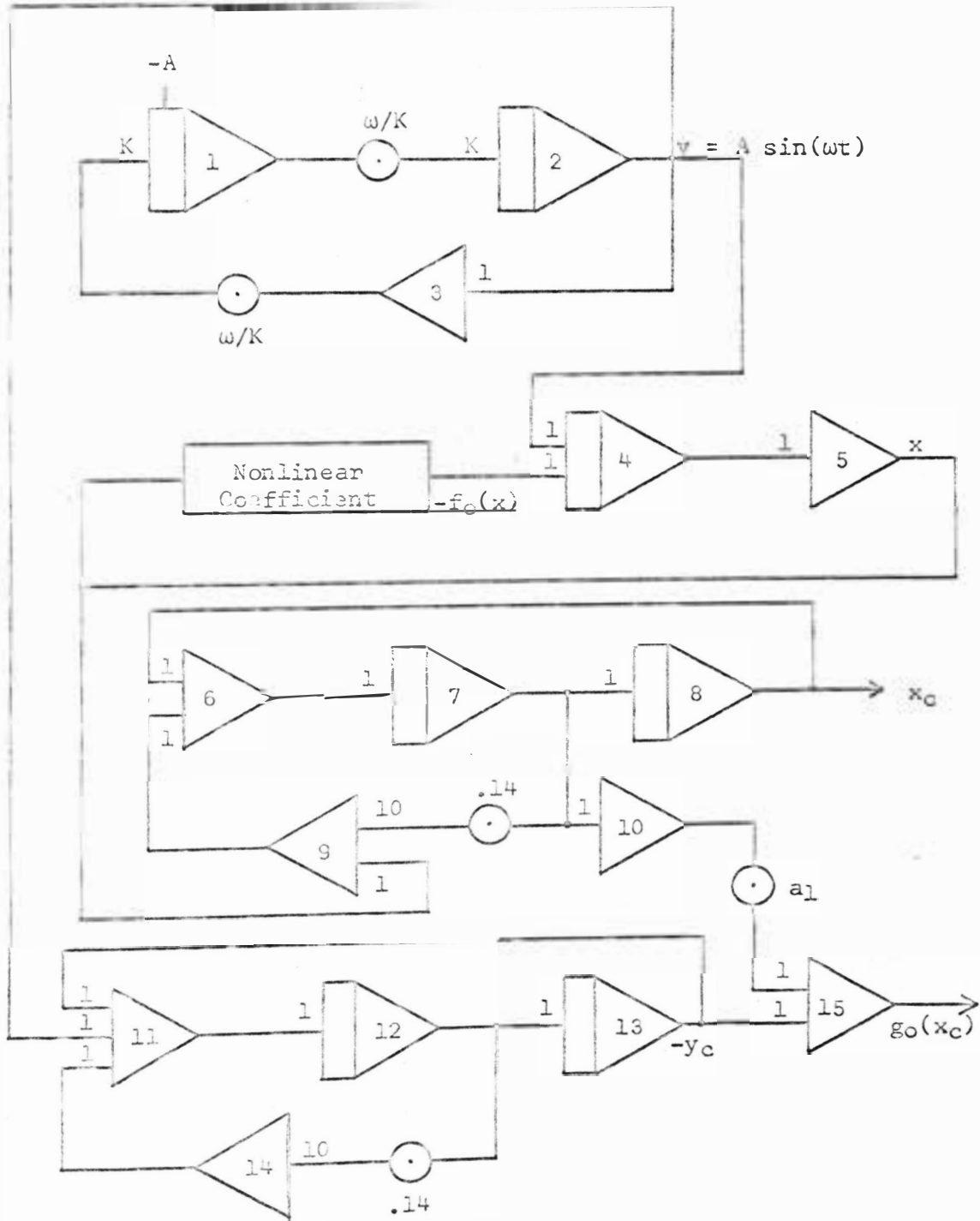


Fig. A-1. Simulation scheme for the identification of first-order nonlinear system.

## APPENDIX B

## SIMULATION OF VARIOUS NONLINEARITIES

## 1. Limiting Type Nonlinearity.

When  $e_1 > e_1 > e_2$ , neither diode conducts and the circuit shown in Fig. B-1 behaves as a linear amplifier with a gain of  $-\frac{R_2}{R_1}$ .

When  $e_1 > e_1$ , diode  $D_1$  conducts and a low-impedance feedback path is established, reducing the amplifier gain to almost zero. Hence the output remains essentially a constant at  $-e_1$ .

When  $e_1 < e_2$ , diode  $D_2$  conducts and the output is about  $+e_2$ .

In both these cases the output levels are not exactly  $-e_1$  or  $+e_2$ , due to the drop in the diodes. Normally the drop in the diodes is negligible. But for precise simulation, the drop should be taken into consideration and compensated.

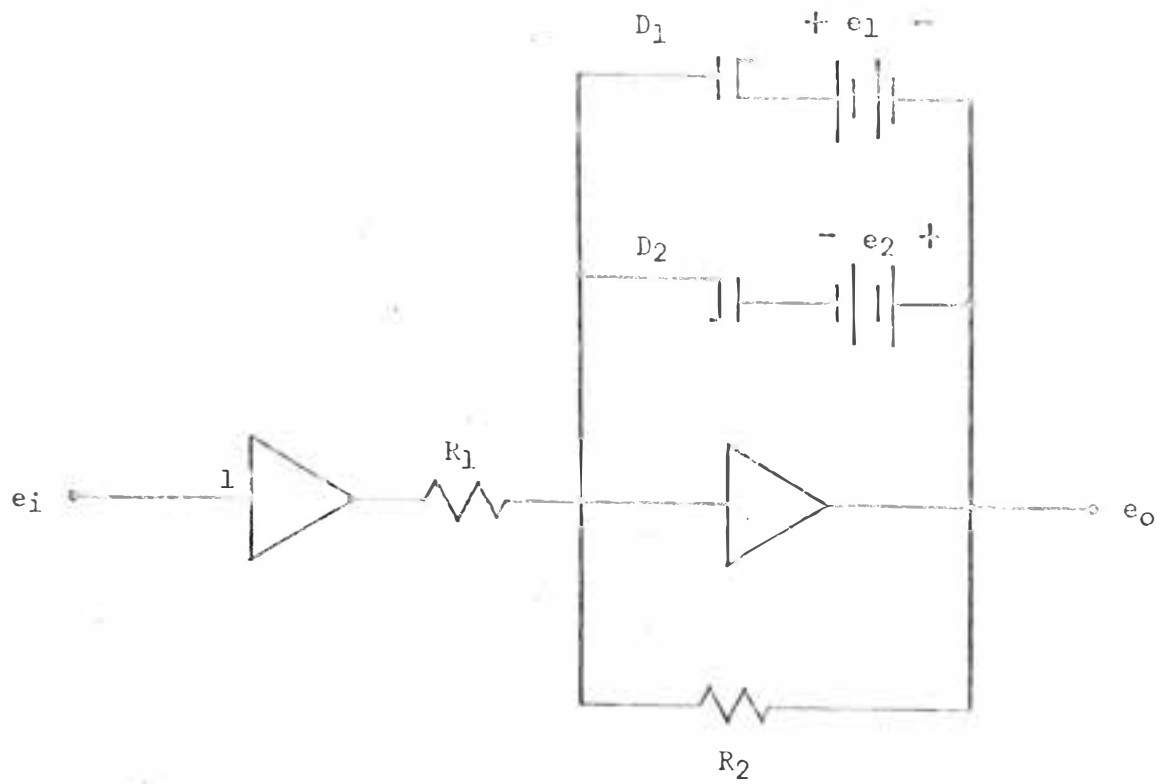


Fig. B-1. Simulation of limiting type nonlinearity.

## 2. Dead Zone Type Nonlinearity.

Fig. B-2 shows the basic circuit used to simulate dead zone type of nonlinearity. The circuit operates as follows:

When  $e_i < e_1$ , only diode  $D_1$  conducts and

$$\begin{aligned} e_o &= \frac{R_4}{R_1 + R_3} e_i + \frac{R_4}{R_1 + R_3} (e_i - e_1) \\ &= \frac{R_4}{R_1 + R_3} + \frac{R_4}{R_1 + R_3} e_i - \frac{R_4}{R_1 + R_3} e_1 \end{aligned} \quad (21)$$

When  $e_i > e_2$ , only diode  $D_2$  conducts and

$$\begin{aligned} e_o &= \frac{R_4}{R_1 + R_3} e_i + \frac{R_4}{R_2 + R_3} (e_i - e_2) \\ &= \frac{R_4}{R_1 + R_3} + \frac{R_4}{R_2 + R_3} e_i - \frac{R_4}{R_2 + R_3} e_2 \end{aligned} \quad (22)$$

When  $e_1 \leq e_i \leq e_2$ , neither diode  $D_1$  nor diode  $D_2$  conducts and

hence,

$$e_o = \frac{R_4}{R_1 + R_3} e_i \quad (23)$$

When  $R_1 = \infty$ , while  $R_2$ ,  $R_3$ , and  $R_4$  are finite, it corresponds to a circuit simulating dead zone; that is, zero output when the input  $e_i$  remains between  $e_1$  and  $e_2$ . When the input is outside these limits, the output is given either by (21) or by (22).



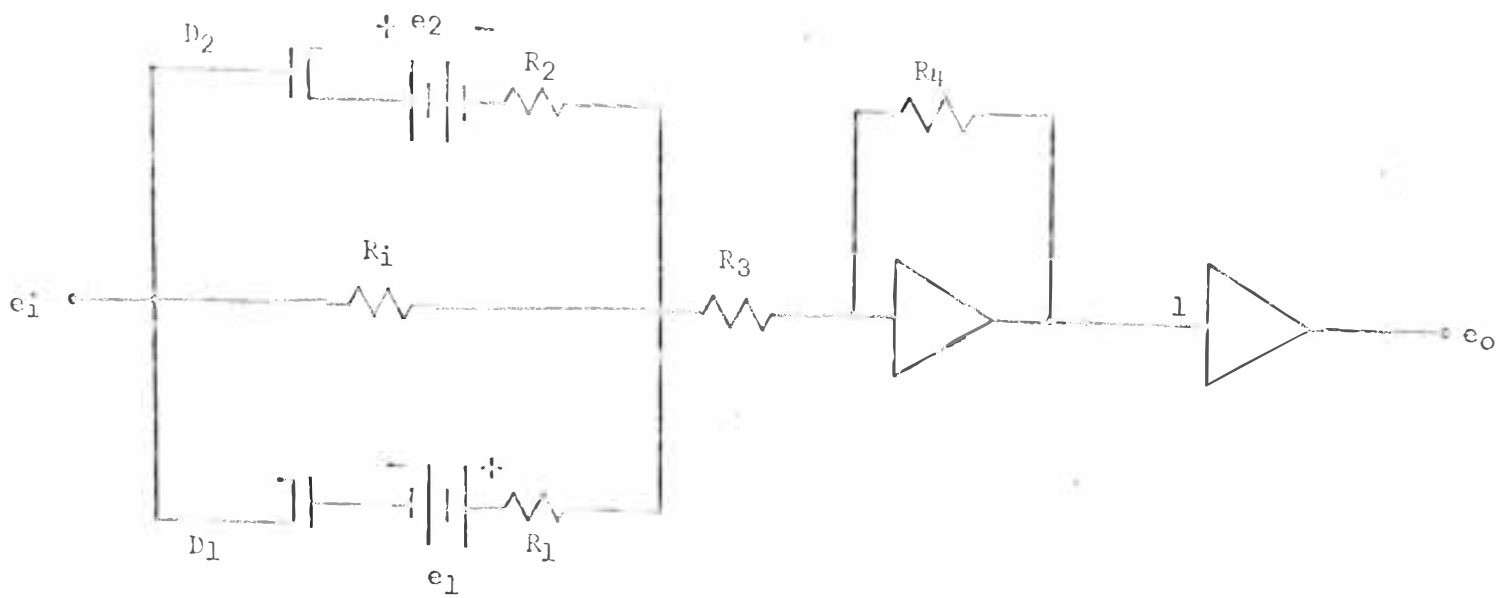


Fig. B-2. Simulation of dead zone.

### 3. Coulomb Friction Type Nonlinearity.

When  $e_2 > e_1 > 0$ , the circuit shown in Fig. B-3 behaves as an operational amplifier with an infinite gain (since the feedback impedance is infinite) and the output  $e_0$  attempts to become infinitely negative. While attempting to become infinitely negative, the output  $e_0$  causes diode  $D_2$  to conduct and thereby establishes a low impedance feedback path through the diode  $D_2$ . Hence, the output level remains clamped at  $-e_2$ .

When  $e_1 > e_2$ , diode  $D_2$  conducts and the output remains at  $-e_2$ .

When  $e_1 < 0$ , the operation may be explained similarly. The difference being diode  $D_1$  conducts instead of diode  $D_2$  and the output remains at  $+e_1$  instead of  $-e_2$ .

When  $|e_1| = |e_2|$ , the circuit simulates coulomb friction where  $e_1$  represents the velocity of the system and  $e_0$  the coulomb friction.

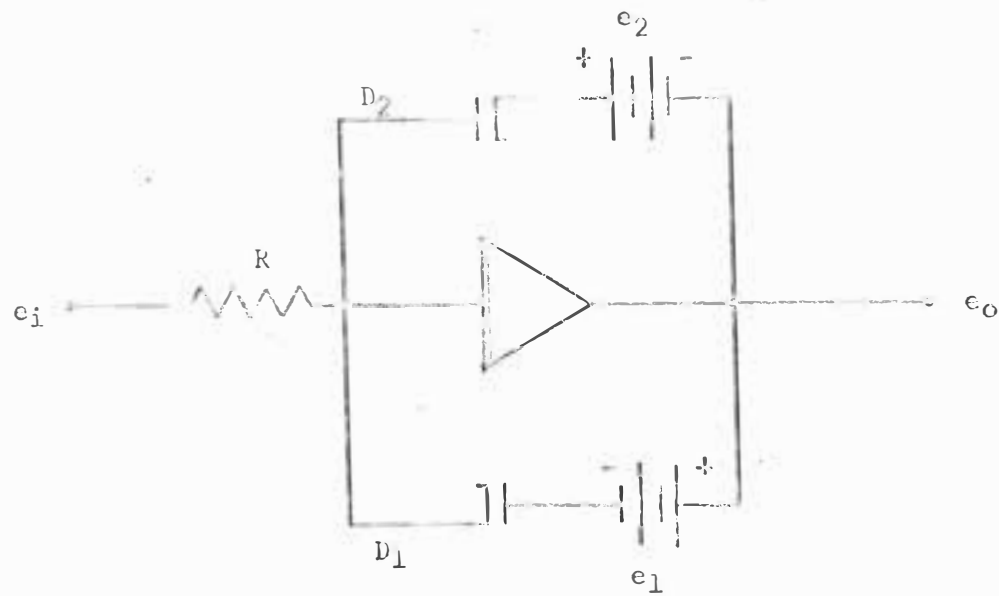


Fig. B-3. Simulation of Coulomb friction.

#### 4. Simulation of Backlash.

The operation of the circuit shown in Fig. B-4 is as follows:

Assuming that the charges on  $C_1$  and  $C_2$  are zero at time  $t = 0$  and that  $C_1 = C_2$ , then so long as  $e_1 < e_i < e_2$ , neither  $D_1$  nor  $D_2$  will conduct and  $e_o = 0$ .

When  $e_i$  exceeds  $e_2$ , then  $D_2$  will conduct and condensers  $C_1$  and  $C_2$  will charge to the voltage  $e_i - e_2$ ; hence,  $e_o = K(e_i - e_2)$ . This relation obtains until  $e_i$  reaches  $e_{i_{max}}$  and reverses direction. The final voltage across the condensers is  $(e_{i_{max}} - e_2)$ , giving an output of  $e_o = K(e_{i_{max}} - e_2)$ .

As  $e_i$  decreases from its maximum value,  $e_o$  remains constant until  $e_i$  reaches the value  $e_1 + (e_{i_{max}} - e_2)$  or  $e_{i_{max}} - (e_2 - e_1)$ , because until  $e_i$  reaches this value condensers  $C_1$  and  $C_2$  have no discharge path. When  $e_i$  reaches this value,  $D_1$  conducts and  $C_1$  and  $C_2$  are discharged to the point where the cathode of  $D_1$  is negative with respect to the plate. Hence, the voltage across  $C_1$  and  $C_2$  is given by  $e_c = e_i - e_1$  and the output by  $e_o = K(e_i - e_1)$ . This relation holds until  $e_i$  reaches  $e_{i_{min}}$ . A positive increase in  $e_i$  yields  $e_o = K(e_{i_{min}} - e_1)$  until  $e_i$  reaches  $e_2 + (e_{i_{min}} - e_1)$ , causing  $D_2$  to conduct and the output  $e_o = K(e_i - e_2)$ . A table of  $e_o$  vs  $e_i$  is given below as  $e_i$  goes through a complete cycle:

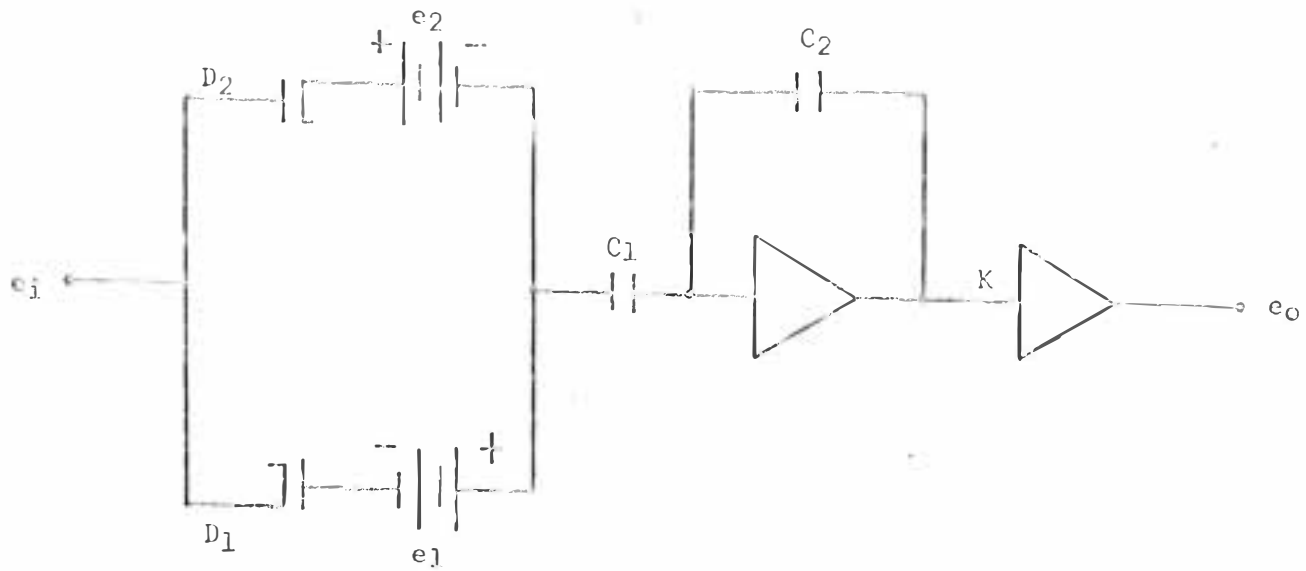


Fig. B-4. Simulation of backlash.

<u><math>e_i</math></u>	<u><math>e_0</math></u>
1. $0 \leq e_i \leq e_2$	0
2. $e_2 < e_i < e_{i\max}$	$K(e_i - e_2)$
3. $(e_1 + e_{i\max} - e_2) < e_i < e_{i\max}$	$K(e_{i\max} - e_2)$
4. $e_{i\min} < e_i < e_1 + (e_{i\max} - e_2)$	$K(e_i - e_1)$
5. $e_{i\min} < e_i < e_2 + (e_{i\min} - e_1)$	$K(e_{i\min} - e_1)$
6. $e_2 + (e_{i\min} - e_1) \leq e_i \leq e_2$	$K(e_i - e_2)$

### 5. Simulation of Relay with Hysteresis.

The operation of this circuit (Fig. B-5) may be explained as follows. For  $e_i$  sufficiently positive, output of amplifier 1 will be  $-e_2$  and  $e_o$  will be  $+e_2$ . Then  $e_3$  will be  $+ae_2$ . As  $e_i$  decreases and reaches  $-ae_2$ , the output of amplifier 1 switches. For more negative  $e_i$  values, output of amplifier 1 will be at  $+e_1$ , and  $e_o$  is at  $-e_1$ . Hence  $e_3$  will be  $-ae_1$ . Increasing  $e_i$  now causes no change until  $e_i$  is equal to  $+ae_1$  and amplifier 1 switches to its negative limit again. When  $|e_1| = |e_2|$ , the nonlinearity is symmetrical.

The output,  $e_o$ , is given by the following table as  $e_i$  goes through a complete cycle:

	<u><math>e_i</math></u>	<u><math>e_o</math></u>
1.	$e_i > 0$	$+e_2$
2.	$e_i \leq -ae_2$	$-e_1$
3.	$ae_1 > e_i > -ae_2$	$-e_1$
4.	$e_i \geq ae_1$	$+e_2$

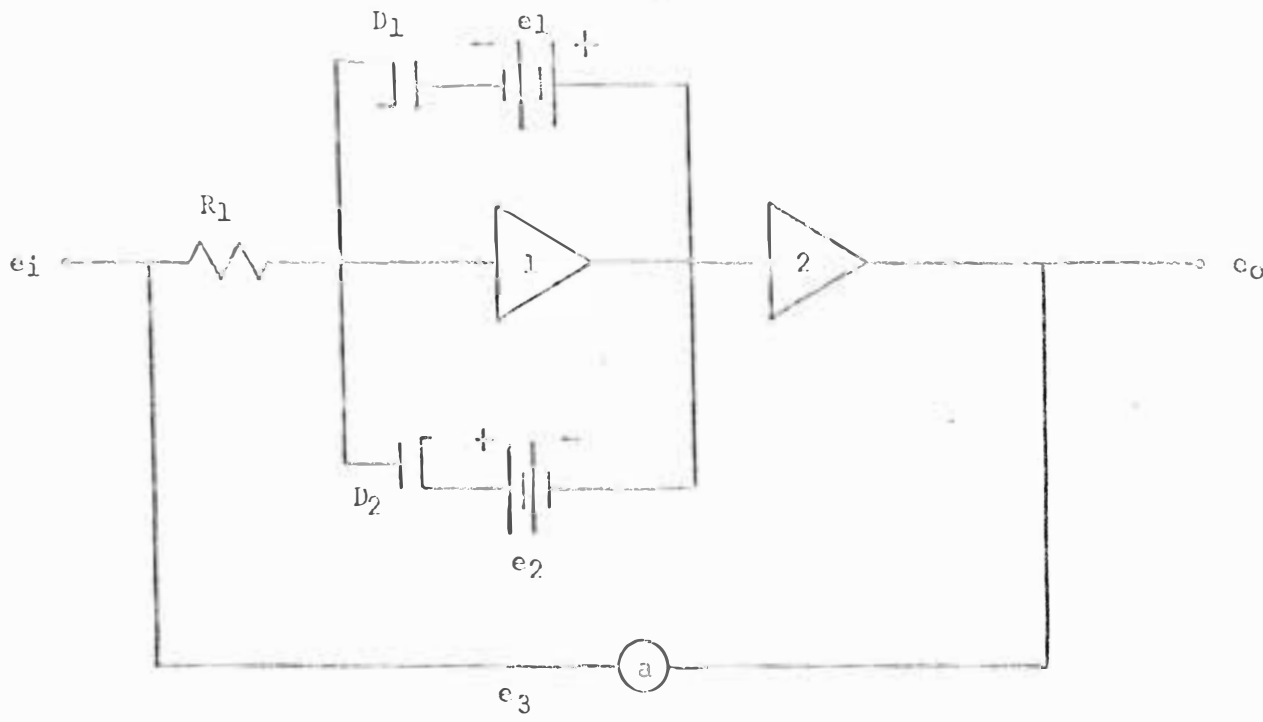


Fig. B-5. Simulation of relay with hysteresis.



## APPENDIX C

Table 1. The Minimum ITAE Standard Forms, Zero-Displacement Error Systems.

---



---


$$S + 1$$

$$S^2 + 1.4S + 1$$

$$S^3 + 1.75S^2 + 2.15S + 1$$

$$S^4 + 2.1S^3 + 3.4S^2 + 2.7S + 1$$

$$S^5 + 2.8S^4 + 5.0S^3 + 5.5S^2 + 3.4S + 1$$

$$S^6 + 3.25S^5 + 6.6S^4 + 8.6S^3 + 7.45S^2 + 3.95S + 1$$

$$S^7 + 4.47S^6 + 10.42S^5 + 15.08S^4 + 15.54S^3 + 10.64S^2 + 4.56S + 1$$

$$S^8 + 5.2S^7 + 12.8S^6 + 21.6S^5 + 25.75S^4 + 22.2S^3 + 13.3S^2 + 5.15S + 1$$


---



---

Table 2. The Butterworth Standard Forms.

---



---


$$S + 1$$

$$S^2 + 1.4S + 1$$

$$S^3 + 2.0S^2 + 2.0S + 1$$

$$S^4 + 2.6S^3 + 3.4S^2 + 2.6S + 1$$

$$S^5 + 3.24S^4 + 5.24S^3 + 5.24S^2 + 3.24S + 1$$

$$S^6 + 3.86S^5 + 7.46S^4 + 9.13S^3 + 7.46S^2 + 3.86S + 1$$

$$S^7 + 4.5S^6 + 10.1S^5 + 14.6S^4 + 14.6S^3 + 10.1S^2 + 4.5S + 1$$

$$S^8 + 5.12S^7 + 13.14S^6 + 21.84S^5 + 25.69S^4 + 21.84S^3 + 13.14S^2 + 5.12S + 1$$


---



---